Space–Time Block Codes Achieving Full Diversity With Linear Receivers

Yue Shang and Xiang-Gen Xia, *Senior Member, IEEE*

***Abstract*—In most of the existing space–time code designs, achieving full diversity is based on maximum-likelihood (ML) decoding at the receiver that is usually computationally expensive and may not have soft outputs. Recently, Zhang–Liu–Wong introduced Toeplitz codes and showed that Toeplitz codes achieve full diversity when a linear receiver, zero-forcing (ZF) or minimum mean square error (MMSE) receiver, is used. Motivated from Zhang–Liu–Wong's results on Toeplitz codes, in this paper, we propose a design criterion for space–time block codes (STBC), in which information symbols and their complex conjugates are linearly embedded, to achieve full diversity when ZF or MMSE receiver is used. The (complex) orthogonal STBC (OSTBC) satisfy the criterion as one may expect. We also show that the symbol rates of STBC under this criterion are upper bounded by 1. Subsequently, we propose a novel family of STBC that satisfy the criterion and thus achieve full diversity with ZF or MMSE receiver. Our newly proposed STBC are constructed by overlapping the 2×2 Alamouti code and hence named overlapped Alamouti codes in this paper. The new codes are close to orthogonal and their symbol rates can approach 1 for any number of transmit antennas. Simulation results show that overlapped Alamouti codes significantly outperform Toeplitz codes for all numbers of transmit antennas and also outperform OSTBC when the number of transmit antennas is above 4.**

***Index Terms*—Full diversity, linear receivers, multiple-input multiple-output (MIMO) systems, minimum mean square error (MMSE), orthogonal space–time block codes, overlapped Alamouti codes, space–time block codes, Toeplitz codes, zero-forcing (ZF).**

I. Introduction

SPACE-TIME codes have been extensively studied in recent years since the early works [1]–[4]. Most of the studies on space–time code designs are based on the criteria obtained in [2], [3], namely full rank/diversity criterion and large diversity product (coding gain or distance product) criterion, and the full diversity criterion is the first one needed to be satisfied since it governs the exponential in the pairwise error probability (PEP) decay vs. the signal-to-noise ratio (SNR). These criteria obtained in [2] and [3] are, however, based on maximum-likelihood (ML) decoding at the receiver that usually has a high complexity and may not have soft outputs. In a practical multiple-input multiple-output (MIMO) system, decoding complexity is an important concern and a decoding scheme with low complexity is always desired. A natural question, then, is whether a space–time code can achieve full diversity when a suboptimal receiver that has low decoding complexity, such as a linear receiver, is used. Unfortunately, most of the existing space–time codes, except orthogonal type codes [4]−[19], may not achieve full diversity when a linear receiver is used, which is not surprising since they are not designed in terms of linear receivers. For (complex) orthogonal space–time block codes (OSTBC), due to the orthogonality of the codes, their maximum likelihood (ML) decoding is already linear and hence they achieve full diversity with linear receivers. However, the symbol rates of OSTBC (with or without linear processing) were shown in [7] to be upper bounded by $3/4$ for more than two transmit antennas and furthermore, a tight upper bound was conjectured to be $(k+1)/(2k)$ for $2k$ or $2k-1$ transmit antennas in [7]. To improve symbol rates, in [12]–[14], quasi-orthogonal STBC (QOSTBC) were introduced for which the orthogonality is relaxed and decoding complexity is hence increased. But the rates of QOSTBC are ultimately limited by the rates of OSTBC. Recently, in [20], [21] by Zhang–Liu–Wong, a family of space–time block codes (STBC) called *Toeplitz codes* was introduced and it was shown that Toeplitz codes achieve full diversity in a multiple-input–single-output (MISO) system when zero-forcing (ZF) or minimum mean square error (MMSE) receiver is used. For Toeplitz codes, although their symbol rates approach 1 as the block sizes go to infinity for any number of transmit antennas, their performance degrades dramatically when the rates or block sizes increase.

Motivated from Zhang–Liu–Wong's results on Toeplitz codes, in this paper, we propose a design criterion for STBC, in which information symbols and their complex conjugates are linearly embedded,[1] to achieve full diversity when an MIMO system is equipped with a linear receiver, specifically, ZF or MMSE receiver. A general OSTBC satisfies the proposed criterion as expected. We also show that the symbol rates of STBC under this criterion are upper bounded by 1. Subsequently, we propose a novel family of STBC that satisfy the criterion and thus achieve full diversity with ZF or MMSE receiver. Our newly proposed STBC are constructed by overlapping the

Manuscript received February 7, 2007; revised February 29, 2008. Current version published September 17, 2008. This work was supported in part by the Air Force Office of Scientific Research (AFOSR) under Grants FA9550-05-1-0161 and FA9550-08-1-0219, and the National Science Foundation under Grant CCR-0325180. The material in this paper was presented in part at the IEEE International Symposium on Information Theory (ISIT'07), Nice, France, June 2007 and the IEEE Global Communications Conference (GLOBECOM'07), Washington, DC, November 2007.

The authors are with the Department of Electrical and Computer Engineering, University of Delaware, Newark, DE 19716 USA (e-mail: shang@ee.udel.edu; xxia@ee.udel.edu).

Communicated by S. W. McLaughlin, Associate Editor for Coding Techniques.

Digital Object Identifier 10.1109/TIT.2008.928986

[1]They can be treated as linear dispersion codes [22], [23] when the real and imaginary parts of information symbols are treated separately.

0018-9448/$25.00 © 2008 IEEE

2×2 Alamouti code and hence named overlapped Alamouti codes in this paper. The symbol rates of overlapped Alamouti codes are slightly higher than those of Toeplitz codes and also approach 1 as the block sizes go to infinity for any number of transmit antennas. Simulation results show that overlapped Alamouti codes significantly outperform Toeplitz codes for all numbers of transmit antennas and also outperform OSTBC when the number of transmit antennas is above 4.

For the existing linear dispersion codes [22], [23], for example, linear lattice based STBC and BLAST, simplified decoding algorithms have been explored in the literature, which include, for example, sphere decoding [24]–[31] and soft (and successive) interference cancellation (SIC) methods [32]–[42], [52]. Although sphere decoding can approach ML decoding performance and thus does not sacrifice the full diversity property of those existing codes that are designed in terms of ML decoding, its complexity may still be much higher than that of linear receivers. For SIC methods, on the other hand, the available diversity may not be fully exploited, even if STBC are designed with full diversity for ML receiver. Besides sphere decoding and SIC methods, space–time spreading and lattice STBC encoders with MMSE decision feedback equalizer (MMSE-DFE) combined with vector or lattice decoding were proposed in [43] and [44], respectively, to achieve the diversity-multiplexing tradeoff [45] when SNR goes to infinity, where, however, the complexity of vector or lattice decoding may be high when the vector (and constellation size) or lattice dimension is not small.

This paper is organized as follows. In Section II, we describe the system model and propose a criterion (sufficient condition) for STBC to achieve full diversity with linear (ZF and MMSE) receivers. In Section III, we present overlapped Alamouti codes that are shown to satisfy the criterion. Besides the constructions, we also investigate some properties of overlapped Alamouti codes. In Section IV, we provide some simulation results to illustrate the superb performance of our overlapped Alamouti codes relative to some existing STBC, such as, Toeplitz codes, OSTBC, V-BLAST, perfect codes and PLUTO codes. Finally, in Section V, we conclude this paper.

II. System Model and Problem Formulation

In this section, we first describe the general MIMO system model and then propose a criterion for STBC to achieve full diversity with linear receivers by considering an equivalent form of the channel model. As two classes of known STBC achieving full diversity with ZF or MMSE receiver, OSTBC and Toeplitz codes are briefly reviewed to verify the criterion.

A. System Model and Equivalent Channel Model

Consider an MIMO system with M transmit and N receive antennas. From a given constellation $\mathcal{C}$ such as PAM, PSK or QAM that is assumed to have unit energy, L symbols $s_1, s_2, \ldots, s_L$ are chosen randomly and independently to form an input symbol sequence $\mathbf{s} = (s_1, s_2, \ldots, s_L)^t \in \mathcal{C}^L$, where $(\cdot)^t$ denotes the transpose of a matrix/vector. To be transmitted from the M transmit antennas, the L symbols s_i in $\mathbf{s}$ are encoded into a space–time block codeword matrix $X(\mathbf{s})$ of size $T \times M$, following some specific forms (for example, Alamouti code structure), where T is the number of channel uses to transmit a codeword, i.e., the block length. Then, the STBC $\mathcal{X}$ is just the set composed of all the possible $X(\mathbf{s})$, i.e.,

$$\mathcal{X} = \{X(\mathbf{s}), \mathbf{s} = (s_1, s_2, \ldots, s_L)^t \in \mathcal{C}^L\} \tag{1}$$

and the *symbol rate* of $\mathcal{X}$ is defined as $\frac{L}{T}$. The channel coefficient between the mth transmit antenna and the nth receive antennas is denoted by $h_{m,n}$, $1 \le m \le M$, $1 \le n \le N$. In this paper, we consider the channel to be quasi-static Rayleigh flat fading and $h_{m,n}$ is constant during the transmission of each codeword matrix (T channel uses). Then, the channel model is

$$Y = \sqrt{\frac{\rho}{\mu}} X(\mathbf{s}) H + W \tag{2}$$

where $H = (h_{m,n})_{1 \le m \le M, 1 \le n \le N}$ is the $M \times N$ channel matrix that is zero-mean, complex Gaussian distributed with a nonsingular covariance matrix Σ, $W = (w_{t,n})_{1 \le t \le T, 1 \le n \le N}$ is the $T \times N$ noise matrix in which all entries are independently and identically $\mathcal{CN}(0,1)$ (zero-mean, unit variance, complex Gaussian) distributed, and $Y = (y_{t,n})_{1 \le t \le T, 1 \le n \le N}$ is the received signal matrix of size $T \times N$. The entries $h_{m,n}$ of H are assumed to have unit variance, which implies $\mathbb{E}_H\left(tr(H^\dagger H)\right) = MN$, and μ in (2) is a normalization factor such that ρ is the SNR at each receive antenna, where and thereafter $tr(\cdot)$ denotes the trace of a square matrix, $(\cdot)^\dagger$ denotes the transpose conjugate of a matrix and $\mathbb{E}_H(\cdot)$ denotes the expectation over H.

To decode the transmitted symbol sequence $\mathbf{s}$ with a linear receiver, we need to extract $\mathbf{s}$ from $X(\mathbf{s})$. To do so, we introduce the following equivalent channel model through some unitary operations from (2):

$$\mathbf{y} = \sqrt{\frac{\rho}{\mu}} \mathcal{H} \mathbf{s} + \mathbf{w} \tag{3}$$

where $\mathcal{H}$, called equivalent channel matrix, that has L columns, is from H, $\mathbf{y}$ is the equivalent received signal vector and $\mathbf{w}$ is the equivalent noise vector whose components are still independently and identically $\mathcal{CN}(0,1)$ distributed. Note that $\mathbf{y}$ and $\mathcal{H}$ in (3) should not be dependent of $\mathbf{s}$ or W in any form, and the noise term $\mathbf{w}$ in (3) should also be independent of $\mathbf{s}$. Hence, if the channel matrix H in (2) is known at the receiver, then $\mathbf{y}$ and $\mathcal{H}$ in (3) are also known from the corresponding transformations and furthermore, $\mathcal{H}$ is an all-zero matrix if and only if H is an all-zero matrix.

For a given STBC $\mathcal{X}$, if an equivalent channel model (3) holds for single receive antenna case, i.e., $N = 1$, its corresponding version for multiple receive antennas can be easily obtained as follows. Let $Y = (\bar{\mathbf{y}}_1, \bar{\mathbf{y}}_2, \ldots, \bar{\mathbf{y}}_N)$, $H = (\mathbf{h}_1, \mathbf{h}_2, \ldots, \mathbf{h}_N)$ and $W = (\bar{\mathbf{w}}_1, \bar{\mathbf{w}}_2, \ldots, \bar{\mathbf{w}}_N)$, where $\bar{\mathbf{y}}_n$, $\mathbf{h}_n$ and $\bar{\mathbf{w}}_n$ are the nth columns of Y, H and W in (2), respectively. When there is only one receive antenna, $Y = \bar{\mathbf{y}}_1$, $H = \mathbf{h}_1$, $W = \bar{\mathbf{w}}_1$ and the channel model is simplified to

$$\bar{\mathbf{y}}_1 = \sqrt{\frac{\rho}{\mu}} X(\mathbf{s}) \mathbf{h}_1 + \bar{\mathbf{w}}_1 \tag{4}$$

which can be reformulated into an equivalent channel model

$$\mathbf{y}_1 = \sqrt{\frac{\rho}{\mu}} \mathcal{H}_1 \mathbf{s} + \mathbf{w}_1 \tag{5}$$

as assumed. For the same code in the system with multiple receive antennas, we have $\bar{\mathbf{y}}_n = \sqrt{\frac{\rho}{\mu}}X(\mathbf{s})\mathbf{h}_n + \bar{\mathbf{w}}_n$ corresponding to the nth receive antenna and its equivalent form is automatically $\mathbf{y}_n = \sqrt{\frac{\rho}{\mu}}\mathcal{H}_n\mathbf{s} + \mathbf{w}_n$, where $\mathbf{y}_n, \mathcal{H}_n$ and $\mathbf{w}_n$ have the same form as $\mathbf{y}_1, \mathcal{H}_1$ and $\mathbf{w}_1$ in (5), respectively, $n = 1, 2, \ldots, N$. Then, the equivalent channel model (3) for $\mathcal{X}$ when $N \geq 1$ can be obtained by stacking $\{\mathbf{y}_n\}$, $\{\mathcal{H}_n\}$ and $\{\mathbf{w}_n\}$, i.e., letting $\mathbf{y} = (\mathbf{y}_1^t, \mathbf{y}_2^t, \ldots, \mathbf{y}_N^t)^t$, $\mathcal{H} = (\mathcal{H}_1^t, \mathcal{H}_2^t, \ldots, \mathcal{H}_N^t)^t$ and $\mathbf{w} = (\mathbf{w}_1^t, \mathbf{w}_2^t, \ldots, \mathbf{w}_N^t)^t$. Note that $\mathbf{w}_n$ is from $\bar{\mathbf{w}}_n$ and $\{\bar{\mathbf{w}}_n\}$ are independent with each other, so are $\{\mathbf{w}_n\}$. Then, the components of $\mathbf{w}$ are independently and identically $\mathcal{CN}(0, 1)$ distributed, as required in model (3).

In the rest of this paper, we mainly focus on the system with single receive antenna, i.e., the MISO system, to study the full diversity property of STBC with linear receivers and the reason will be clear in Section II-B. To simplify the expression, we rewrite (4) for the MISO channel into the following form:

$$\bar{\mathbf{y}} = \sqrt{\frac{\rho}{\mu}}X(\mathbf{s})\mathbf{h} + \bar{\mathbf{w}} \tag{6}$$

by omitting the subscript index for receive antennas, where $\mathbf{h} = (h_1, h_2, \ldots, h_M)^t$ is the channel matrix (vector) and $\bar{\mathbf{y}} = (y_1, y_2, \ldots, y_T)^t$ and $\bar{\mathbf{w}} = (w_1, w_2, \ldots, w_T)^t$ are received signal vector and noise vector, respectively.

The existence of an equivalent channel model (3) depends on the structure of the STBC $\mathcal{X}$. A simple observation that will be used in Section III is that if each row (corresponding to a channel use) of $X(\mathbf{s})$ has its transmitted symbols all in the form of $\pm s_l$ or, alternatively, all in the form of $\pm s_l^*$, then the reformulation from (2) to (3) is feasible, where $(\cdot)^*$ denotes the conjugate of a scalar/matrix. For example, for the Alamouti code [4] in the form of

$$X(\mathbf{s}) = \begin{pmatrix} s_1 & s_2 \\ -s_2^* & s_1^* \end{pmatrix}$$

where $\mathbf{s} = (s_1, s_2)^t$, we have the channel model

$$\begin{pmatrix} y_1 \\ y_2 \end{pmatrix} = \sqrt{\frac{\rho}{2}} \begin{pmatrix} s_1 & s_2 \\ -s_2^* & s_1^* \end{pmatrix} \begin{pmatrix} h_1 \\ h_2 \end{pmatrix} + \begin{pmatrix} w_1 \\ w_2 \end{pmatrix} \tag{7}$$

from (6) for single receive antenna, which is equivalent to

$$\begin{pmatrix} y_1 \\ y_2^* \end{pmatrix} = \sqrt{\frac{\rho}{2}} \begin{pmatrix} h_1 & h_2 \\ h_2^* & -h_1^* \end{pmatrix} \begin{pmatrix} s_1 \\ s_2 \end{pmatrix} + \begin{pmatrix} w_1 \\ w_2^* \end{pmatrix}. \tag{8}$$

However, such a structure is not common for STBC and it has been shown in [11] that the rates of the square OSTBC that have this structure are upper bounded by $\frac{2}{M}$ for even number of transmit antennas and $\frac{1}{M}$ for odd number of transmit antennas, respectively. So, imposing such a special format on OSTBC may induce rate losses, while their equivalent channel models can be easily derived. Fortunately, the reformulation from (2) to (3) is not only restricted to this special case.

For a general OSTBC, we can express its codeword matrix as $X(\mathbf{s}) = (A_1\mathbf{s} + B_1\mathbf{s}^*, A_2\mathbf{s} + B_2\mathbf{s}^*, \ldots, A_M\mathbf{s} + B_M\mathbf{s}^*)$ with A_i and B_i being $T \times L$ complex-valued constant matrices, $i = 1, 2, \ldots, M$. From (6), we multiply its both sides by $\sum_{i=1}^M h_i^* A_i^\dagger$ and also the conjugates of its both sides by $\sum_{i=1}^M h_i B_i^t$, and sum the two resulting equations. It can be derived from the Radon-Hurwitz equalities on $\{A_i, B_i\}$ that the equivalent channel model corresponding to (6) for OSTBC is

$$\mathbf{y} = \sqrt{\frac{\rho}{\mu}}\|\mathbf{h}\|\mathbf{s} + \mathbf{w} \tag{9}$$

where $\mathbf{y} = \|\mathbf{h}\|^{-1}\left(\sum_{i=1}^M \left(h_i^* A_i^\dagger \bar{\mathbf{y}} + h_i B_i^t \bar{\mathbf{y}}^*\right)\right)$, $\mathbf{w} = \|\mathbf{h}\|^{-1}\left(\sum_{i=1}^M \left(h_i^* A_i^\dagger \bar{\mathbf{w}} + h_i B_i^t \bar{\mathbf{w}}^*\right)\right) \sim \mathcal{CN}(0, I_L)$, and $\|\cdot\|$ and I_L denote the norm[2] of a matrix and the identity matrix of dimension L, respectively. The model in (9) is intuitive as it is well known that the orthogonality of an OSTBC completely decouples an MIMO channel into many parallel and independent subchannels.

In [20] and [21], Zhang–Liu–Wong introduced a class of STBC called Toeplitz codes that can achieve full diversity with linear receivers in an MISO system. Using the notations in [20], [21], we write $T(\mathbf{v}, p, q)$ to denote a Toeplitz matrix of size $(p + q - 1) \times q$ as follows:

$$T(\mathbf{v}, p, q) = \begin{pmatrix} v_1 & 0 & \ldots & 0 \\ v_2 & v_1 & \ldots & 0 \\ v_3 & v_2 & \ldots & 0 \\ \vdots & \vdots & \ddots & \vdots \\ v_p & v_{p-1} & \ldots & v_1 \\ 0 & v_p & \ldots & v_2 \\ \vdots & \vdots & \ddots & \vdots \\ 0 & 0 & \ldots & v_p \end{pmatrix} \tag{10}$$

where $\mathbf{v} = (v_1, v_2, \ldots, v_p)^t$ is any vector of length p. A Toeplitz code with L symbols embedded in each codeword matrix that are transmitted from M antennas is then defined as

$$\mathcal{T}_{M,L} = \{T(\mathbf{s}, L, M), \mathbf{s} = (s_1, s_2, \ldots, s_L)^t \in \mathcal{C}^L\}. \tag{11}$$

The rate of $\mathcal{T}_{M,L}$ is

$$R_{\mathcal{T}_{M,L}} = \frac{L}{L + M - 1} \tag{12}$$

that approaches 1 as L goes to infinity for a fixed number of transmit antennas. In fact, the above Toeplitz codes are delay diversity codes [1], [3] if they are treated as trellis codes. From (6) for single antenna at the receiver, the channel model for the Toeplitz code $\mathcal{T}_{M,L}$ is $\bar{\mathbf{y}} = \sqrt{\frac{\rho}{\mu}}T(\mathbf{s}, L, M)\mathbf{h} + \bar{\mathbf{w}}$, which is easily reformulated into the following equivalent channel model

$$\underbrace{\bar{\mathbf{y}}}_{\mathbf{y}} = \sqrt{\frac{\rho}{\mu}}\underbrace{T(\mathbf{h}, M, L)}_{\mathcal{H}}\mathbf{s} + \underbrace{\bar{\mathbf{w}}}_{\mathbf{w}} \tag{13}$$

where the equivalent channel matrix $\mathcal{H}$ is still a Toeplitz matrix $T(\mathbf{h}, M, L)$.

[2]The norm of a matrix in this paper is referred to the Frobenius norm, i.e., $\|A\| = \left(\sum_{i=1}^r \sum_{j=1}^c |a_{i,j}|^2\right)^{\frac{1}{2}}$ for matrix $A = (a_{i,j})_{1 \leq i \leq r, 1 \leq j \leq c}$.

B. A Criterion for STBC to Achieve Full Diversity With Linear Receivers

The equivalent channel model (3) acts as the basis for linear decoding. Specifically, for ZF receiver, the estimate $\hat{\mathbf{s}}_{ZF}$ of the transmitted symbol sequence $\mathbf{s}$ is, if $(\mathcal{H}^\dagger\mathcal{H})^{-1}$ exists,

$$\hat{\mathbf{s}}_{ZF} = \sqrt{\frac{\mu}{\rho}}(\mathcal{H}^\dagger\mathcal{H})^{-1}\mathcal{H}^\dagger\mathbf{y} = \mathbf{s} + \sqrt{\frac{\mu}{\rho}}(\mathcal{H}^\dagger\mathcal{H})^{-1}\mathcal{H}^\dagger\mathbf{w} \quad (14)$$

and for MMSE receiver, the estimate is

$$\begin{aligned}\hat{\mathbf{s}}_{MMSE} &= \sqrt{\frac{\rho}{\mu}}\left(I_L + \frac{\rho}{\mu}\mathcal{H}^\dagger\mathcal{H}\right)^{-1}\mathcal{H}^\dagger\mathbf{y} \\ &= \frac{\rho}{\mu}\left(I_L + \frac{\rho}{\mu}\mathcal{H}^\dagger\mathcal{H}\right)^{-1}\mathcal{H}^\dagger\mathcal{H}\mathbf{s} \\ &\quad + \sqrt{\frac{\rho}{\mu}}\left(I_L + \frac{\rho}{\mu}\mathcal{H}^\dagger\mathcal{H}\right)^{-1}\mathcal{H}^\dagger\mathbf{w} \qquad (15)\end{aligned}$$

where $(\cdot)^{-1}$ denotes the inverse of a square matrix. It is well-known that MMSE receiver is superior to or, at least, equivalent to ZF receiver. So, if an STBC $\mathcal{X}$ in (1) can achieve full diversity with ZF receiver, so can it with MMSE receiver.

The components of the above ZF or MMSE solution, i.e., $\hat{\mathbf{s}}_{ZF}$ or $\hat{\mathbf{s}}_{MMSE}$, can be treated as the soft outputs of the information symbols in $\mathbf{s}$, when there is an outer error correcting decoder. With component-wise hard decision at ZF or MMSE receiver, the following theorem provides a criterion for STBC to achieve full diversity.

Theorem 1: For PAM, PSK and square QAM constellations, the STBC $\mathcal{X}$ in (1) can achieve full diversity, i.e., the symbol error probability (SEP) $P_e(\hat{s}_l \to s_l)$ of s_l satisfies

$$P_e(\hat{s}_l \to s_l) \le \bar{c}\cdot\rho^{-ML}, \quad l = 1, 2, \ldots, L,$$

for some positive constant $\bar{c}$ that is independent of ρ, with ZF or MMSE receiver, if an equivalent channel matrix $\mathcal{H}$ in (3) exists and satisfies

$$\|\mathcal{H}\| \le g\|H\| \text{ and } \det(\mathcal{H}^\dagger\mathcal{H}) \ge c\|H\|^{2L} \qquad (16)$$

for any realization of the channel matrix H in (2), where $\det(\cdot)$ denotes the determinant of a matrix, g and c are positive constants independent of H, and L is the number of symbols encoded in each codeword matrix of $\mathcal{X}$, i.e., the length of $\mathbf{s}$ in (3).

Its proof is in Appendix A. Notice that a similar condition as that in (16) was introduced and used in the proof of the full diversity property of Toeplitz codes with linear receivers in [20], [21]. Several simple observations can be made immediately from Theorem 1. First, for (16) to be satisfied, all the MN components of H must occur in each column of $\mathcal{H}$ and otherwise, $\mathcal{H}$ may have all-zero columns, inducing $\det(\mathcal{H}^\dagger\mathcal{H}) = 0$, while H is not an all-zero matrix. Second, in order to reduce the interferences between the transmitted symbols s_l, $\mathcal{H}$ should be as orthogonal as possible and once $\mathcal{H}$ is orthogonal, the L symbols s_l are fully decoupled and hence ZF decoder and ML decoder are equivalent. We will discuss this more in Section III. Third, the design criterion (16) does not explicitly depend on the number of receive antennas N, although for different N, $\mathcal{H}$ or H is different. The reason is that once an STBC satisfies the criterion (16) for a special number of receive antennas, say, N_0, so does it for any $N \ne N_0$, i.e., the code can then achieve full diversity with ZF or MMSE receiver for any number of receive antennas. We describe this result in the following corollary.

Corollary 1: Assume an equivalent channel model (3) exists for some STBC $\mathcal{X}$ and the equivalent channel matrix is $\mathcal{H} = (\mathcal{H}_1^t, \mathcal{H}_2^t, \ldots, \mathcal{H}_N^t)^t$ for N receive antennas, where $\mathcal{H}_n$ corresponds to the nth receive antenna, $n = 1, 2, \ldots, N$. Then, $\mathcal{H}$ satisfies the criterion (16) in Theorem 1 for $N > 1$ if and only if $\mathcal{H}$ satisfies (16) for $N = 1$.

Proof: Without loss of generality, we assume the channel matrix $H = (\mathbf{h}_1, \mathbf{h}_2, \ldots, \mathbf{h}_N)$ in (2) is not an all-zero matrix, where $\mathbf{h}_n$ is the nth column of H. When $N = 1$, we have $\mathcal{H} = \mathcal{H}_1$, $H = \mathbf{h}_1$ and the channel model and the equivalent one are given in (4) and (5), respectively. The necessity can be easily proved by setting $\mathbf{h}_2 = \mathbf{h_3} = \cdots = \mathbf{h}_N = 0$ in H, which imposes $\mathcal{H}_2 = \mathcal{H}_3 = \cdots = \mathcal{H}_N = 0$ in $\mathcal{H}$ since $\mathcal{H}_n$ is the equivalent channel matrix corresponding to the nth receive antenna. So, it suffices for us to show the sufficiency.

Assume there exist some positive constants g and c such that $\|\mathcal{H}_1\| \le g\|\mathbf{h}_1\|$ and $\det(\mathcal{H}_1^\dagger\mathcal{H}_1) \ge c\|\mathbf{h}_1\|^{2L}$ for any $\mathbf{h}_1$. For $N > 1$, since the equivalence between $\mathcal{H}_n$ and $\mathbf{h}_n$ is the same as that between $\mathcal{H}_1$ and $\mathbf{h}_1$ and thus $\mathcal{H}_n$ has the same form (structure) as $\mathcal{H}_1$, we know $\|\mathcal{H}_n\| \le g\|\mathbf{h}_n\|$ and $\det\left(\mathcal{H}_n^\dagger\mathcal{H}_n\right) \ge c\|\mathbf{h}_n\|^{2L}$ for any $\mathbf{h}_n$, $n = 1, 2, \ldots, N$. Hence, for any H, we have

$$\begin{aligned}&\|\mathcal{H}\|^2 = \sum_{n=1}^{N}\|\mathcal{H}_n\|^2 \le g^2\sum_{n=1}^{N}\|\mathbf{h}_n\|^2 = g^2\|H\|^2 \\ &\Rightarrow \|\mathcal{H}\| \le g\|H\|.\end{aligned}$$

One the other hand, for any given channel matrix H, we choose n_0 such that $\|\mathbf{h}_{n_0}\| = \max_{1\le n\le N}\|\mathbf{h}_n\|$. Hence, $\|H\| \le \sqrt{N}\|\mathbf{h}_{n_0}\|$ and $\|\mathbf{h}_{n_0}\| > 0$. It is known that if matrices $A_1, A_2, \ldots, A_N$ are positive semidefinite, then [46]

$$\det\left(\sum_{n=1}^{N}A_n\right) \ge \sum_{n=1}^{N}\det(A_n) \ge \det(A_{n_0}) \qquad (17)$$

for $\forall n_0 \in [1, N]$. Since $\mathcal{H}_n^\dagger\mathcal{H}_n$ must be positive semidefinite, we have from (17) that

$$\begin{aligned}\det(\mathcal{H}^\dagger\mathcal{H}) &= \det\left(\sum_{n=1}^{N}\mathcal{H}_n^\dagger\mathcal{H}_n\right) \ge \det\left(\mathcal{H}_{n_0}^\dagger\mathcal{H}_{n_0}\right) \\ &\ge c\|\mathbf{h}_{n_0}\|^{2L} \ge c\left(\frac{\|H\|}{\sqrt{N}}\right)^{2L} \\ &= \frac{c}{N^L}\|H\|^{2L} \qquad (18)\end{aligned}$$

where $\frac{c}{N^L}$ is a positive constant independent of H. Thus, we have completed the proof. □

Corollary 1 tells us that whether (16) holds or not is independent of the number of receive antennas, N, and we can pick any $N \ge 1$ when checking the full diversity property of an STBC with ZF or MMSE receiver through (16). So, without loss of generality, we only need to focus on the channel model (6) for single receive antenna, i.e., an MISO system, in the subsequent

discussions. From Corollary 1, the following corollary is immediate.

Corollary 2: The symbol rates of the STBC that satisfy the criterion (16) in Theorem 1 and thus achieve full diversity with ZF or MMSE receiver can not be above 1, i.e., they are upper bounded by 1.

Proof: Assume an STBC $\mathcal{X}$ satisfies the criterion (16) for N receive antennas with $N \geq 1$ and has symbol rate larger than 1. The solution for ZF receiver is infeasible for $\mathcal{X}$ when there is single receive antenna since in this case, the number of variables s_i is larger than the number of linear equations in (3). Then, $\mathcal{X}$ has no full diversity for single receive antenna with ZF receiver. However, from Corollary 1, we know $\mathcal{X}$ has full diversity with ZF receiver for any number of receive antennas. So, a contradiction results. A similar argument can be applied to MMSE receiver. □

Theorem 1, together with Corollary 1 and Corollary 2, provides a criterion (sufficient condition) for us to construct STBC by designing their equivalent channel matrices such that full diversity can be achieved when the MIMO system is equipped with a linear (ZF or MMSE) receiver. Note that, as ML decoding is always superior to or, at least, equivalent to linear decoding, any STBC satisfying the criterion (16) in Theorem 1 is automatically guaranteed to have full diversity with ML receiver.

To verify the validity of the criterion in Theorem 1, we consider OSTBC and Toeplitz codes in MISO systems. From (9), the equivalent channel matrix for a general OSTBC is $\mathcal{H} = \|\mathbf{h}\| I_L$ that obviously satisfies the criterion (16). For Toeplitz codes $\mathcal{T}_{M,L}$, its equivalent channel matrix is $\mathcal{H} = T(\mathbf{h}, M, L)$ from (13) which meets the first part of the sufficient condition in Theorem 1, i.e., $\|\mathcal{H}\| = g\|\mathbf{h}\|$ with $g = \sqrt{L}$. In [20], [21], Zhang–Liu–Wong showed that the second part of the criterion (16), i.e., $\det(\mathcal{H}^\dagger \mathcal{H})/\|\mathbf{h}\|^{2L} \geq c > 0$ for some constant c, holds for Toeplitz codes. We cite this result in the following lemma that will be utilized in Section III to show overlapped Alamouti codes satisfy the criterion (16).

Lemma 1 (Zhang–Liu–Wong [20], [21]): For any given positive integers M and L, the equivalent channel matrix $\mathcal{H} = T(\mathbf{h}, M, L)$ in (13) for Toeplitz code $\mathcal{T}_{M,L}$ satisfies

$$\det(\mathcal{H}^\dagger \mathcal{H}) \geq c\|\mathbf{h}\|^{2L} \tag{19}$$

for any $\mathbf{h}$, where c is a positive constant independent of $\mathbf{h}$, but may depend on M and L.

According to Lemma 1 and Corollary 1, Toeplitz codes achieve full diversity in an MIMO system when ZF or MMSE receiver is used. In general, an explicit expression of the constant c in (19) that depends on M and L may be difficult to obtain. However, when $M = 2$, c can be explicitly expressed in terms of L as $c = 2^{-L}$, i.e.

$$\det\left(T^\dagger(\mathbf{h}, 2, L) T(\mathbf{h}, 2, L)\right) \geq 2^{-L}\|\mathbf{h}\|^{2L} \tag{20}$$

for any $\mathbf{h} = (h_1, h_2)^t$, and its proof is in Appendix B. Note that the above lower bound may not be tight. For instance, when $M = 2$ and $L = 3$, a tight lower bound for $\det\left(T^\dagger(\mathbf{h}, 2, 3) T(\mathbf{h}, 2, 3)\right)/\|\mathbf{h}\|^6$ is easily shown to be $\frac{1}{2}$ that is much larger than that given in (20), where $2^{-L} = \frac{1}{8}$ for $L = 3$.

III. A New Family of STBC: Overlapped Alamouti Codes

While Toeplitz codes [20], [21] achieve full diversity with linear receivers and have symbol rates approaching 1 as the block sizes go to infinity for any number of transmit antennas, their performance degrades dramatically when the rates or block sizes increase. Although for OSTBC, ZF receiver is already ML receiver due to their orthogonality, their symbol rates are low for more than two transmit antennas. This motivates us to design other STBC that not only satisfy the criterion (16) in Theorem 1 and hence achieve full diversity with ZF or MMSE receiver, but also have performance improvements over Toeplitz codes and OSTBC. A novel family of STBC that meet the above two requirements will be systematically constructed in this section and their properties will also be investigated. Since the codeword matrix of the newly proposed STBC is composed of a sequence of overlapped 2×2 Alamouti codes, we call them as overlapped Alamouti codes.

A. Overlapped Alamouti Codes for Odd Transmit Antennas

We now describe the construction of overlapped Alamouti codes as well as their equivalent channel matrices $\mathcal{H}$ in (3) for odd number of transmit antennas, i.e., M is odd, that is larger than 2. To do so, we need to define two types of matrices that have a similar form as the Toeplitz matrix $T(\mathbf{v}, p, q)$ in (10). First, we define matrix $O(\mathbf{v}, p, q)$ of size $(p + q - 1) \times q$ as

$$O(\mathbf{v}, p, q) = \begin{pmatrix} v_1^* & 0 & \dots & 0 \\ v_2^* & v_1 & \dots & 0 \\ v_3^* & v_2 & \dots & 0 \\ \vdots & \vdots & \ddots & \vdots \\ v_{p-1}^* & v_{p-2} & \dots & v_1^* \\ v_p^* & v_{p-1} & \dots & v_2^* \\ 0 & v_p & \dots & v_3^* \\ \vdots & \vdots & \ddots & \vdots \\ 0 & 0 & \dots & v_p^* \end{pmatrix} \tag{21a}$$

and

$$\begin{pmatrix} v_1^* & 0 & \dots & 0 & 0 \\ v_2^* & v_1 & \dots & 0 & 0 \\ v_3^* & v_2 & \dots & 0 & 0 \\ \vdots & \vdots & \ddots & \vdots & \vdots \\ v_p^* & v_{p-1} & \dots & v_1^* & 0 \\ 0 & v_p & \dots & v_2^* & v_1 \\ \vdots & \vdots & \ddots & \vdots & \vdots \\ 0 & 0 & \dots & v_p^* & v_{p-1} \\ 0 & 0 & \dots & 0 & v_p \end{pmatrix} \tag{21b}$$

for odd and even q, respectively, where $\mathbf{v} = (v_1, v_2, \dots, v_p)^t$ is any vector of length p. We can see that in $O(\mathbf{v}, p, q)$, the vectors $\mathbf{v}^*$ and $\mathbf{v}$ alternatively run through the matrix from the

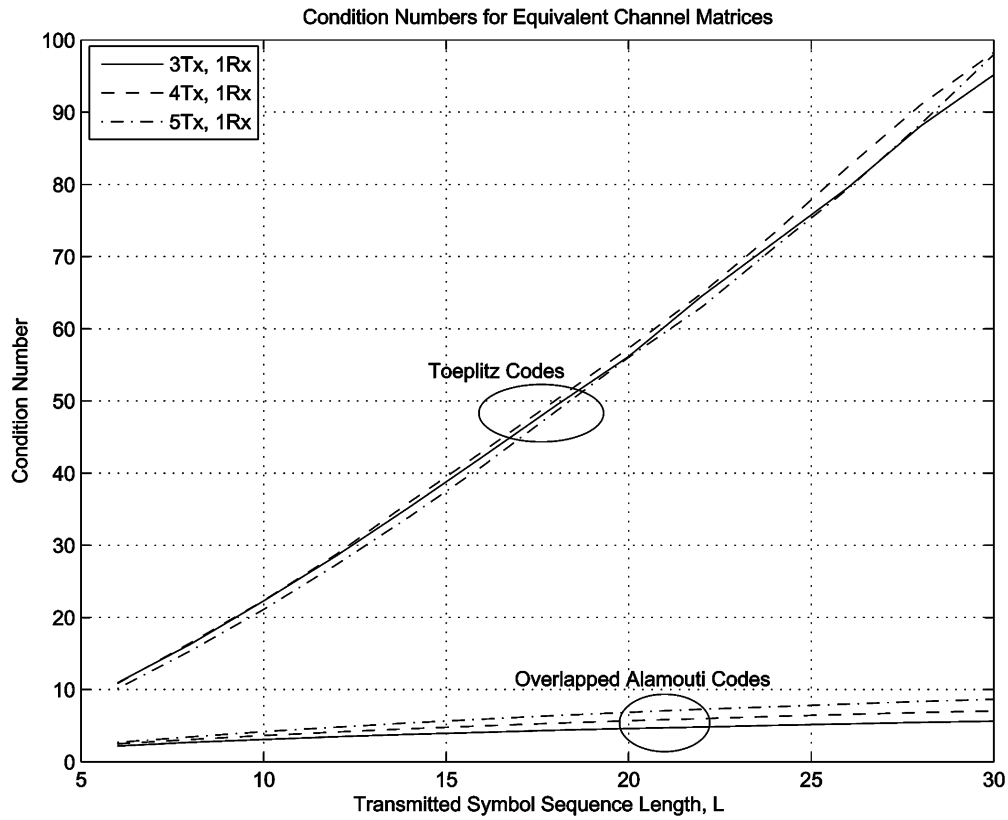

Fig. 1. Comparison of the condition numbers of the matrices $\mathcal{H}^{\dagger}\mathcal{H}$ for overlapped Alamouti codes and Toeplitz codes when the MIMO system is equipped with three, four, and five transmit antennas and one receive antenna.

top-left corner to the bottom-right corner. Second, we define matrix $E(\mathbf{v},p,q)$ of size $(p+q-1)\times q$ as

$$E(\mathbf{v},p,q)=\begin{pmatrix} 0 & \dots & 0 & v_1 \\ 0 & \dots & -v_1^* & v_2 \\ 0 & \dots & -v_2^* & v_3 \\ \vdots & \vdots & \vdots & \vdots \\ v_1 & \dots & -v_{p-2}^* & v_{p-1} \\ v_2 & \dots & -v_{p-1}^* & v_p \\ v_3 & \dots & -v_p^* & 0 \\ \vdots & \vdots & \vdots & \vdots \\ v_p & \dots & 0 & 0 \end{pmatrix} \tag{22a}$$

and

$$\begin{pmatrix} 0 & 0 & \dots & 0 & v_1 \\ 0 & 0 & \dots & -v_1^* & v_2 \\ 0 & 0 & \dots & -v_2^* & v_3 \\ \vdots & \vdots & \vdots & \vdots & \vdots \\ 0 & v_1 & \dots & -v_{p-1}^* & v_p \\ -v_1^* & v_2 & \dots & -v_p^* & 0 \\ \vdots & \vdots & \vdots & \vdots & \vdots \\ -v_{p-1}^* & v_p & \dots & 0 & 0 \\ -v_p^* & 0 & \dots & 0 & 0 \end{pmatrix} \tag{22b}$$

for odd and even q, respectively, where the vectors $\mathbf{v}$ and $-\mathbf{v}^*$ alternatively run through the matrix from the top right corner to the bottom left corner. Furthermore, from the transmitted symbol sequence $\mathbf{s}=(s_1,s_2,\dots,s_L)^t$, we define vectors $\mathbf{s}_o$ and $\mathbf{s}_e$ for odd M as

$$\mathbf{s}_o=\begin{cases}(s_1,0,s_3,0,\dots,0,s_L)^t, & L \text{ odd}, M \text{ odd}\\ (s_1,0,s_3,0,\dots,s_{L-1},0)^t, & L \text{ even}, M \text{ odd}\end{cases} \tag{23}$$

which keeps all the components of $\mathbf{s}$ with odd indices and replace the other components by 0, and correspondingly

$$\mathbf{s}_e=\begin{cases}(0,s_2,0,s_4,\dots,s_{L-1},0)^t, & L \text{ odd}, M \text{ odd}\\ (0,s_2,0,s_4,\dots,0,s_L)^t, & L \text{ even}, M \text{ odd}\end{cases} \tag{24}$$

which instead keeps all the components of $\mathbf{s}$ with even indices. Note that $\mathbf{s}_o$ and $\mathbf{s}_e$ have the same length L as $\mathbf{s}$. Now we are ready to define the codeword matrix of overlapped Alamouti codes for odd M as follows.

For odd M transmit antennas, the codeword matrix $X(\mathbf{s})$ of an overlapped Alamouti code which has L information symbols embedded is defined as

$$X(\mathbf{s})=O(\mathbf{s}_o,L,M)+E(\mathbf{s}_e,L,M) \tag{25}$$

where $\mathbf{s}$ is the transmitted symbol sequence and $\mathbf{s}_o$ and $\mathbf{s}_e$ are defined in (23) and (24), respectively. Then, the corresponding overlapped Alamouti code is

$$\mathcal{O}_{M,L}=\{O(\mathbf{s}_o,L,M)+E(\mathbf{s}_e,L,M), \quad \mathbf{s}=(s_1,s_2,\dots,s_L)^t\in\mathcal{C}^L\} \tag{26}$$

which has symbol rate $R_{\mathcal{O}_{M,L}}=\frac{L}{L+M-1}$, the same as the symbol rate of the Toeplitz code $\mathcal{T}_{M,L}$ in (11).

As an example, when $M=3$, the codeword matrix of $\mathcal{O}_{3,L}$ has the following form:

$$X(\mathbf{s})=\begin{pmatrix} s_1^* & 0 & 0\\ 0 & s_1 & s_2\\ s_3^* & -s_2^* & s_1^*\\ s_2 & s_3 & s_4\\ s_5^* & -s_4^* & s_3^*\\ s_4 & s_5 & s_6\\ \vdots & \vdots & \vdots\\ s_{L-2}^* & -s_{L-3}^* & s_{L-4}^*\\ s_{L-3} & s_{L-2} & s_{L-1}\\ s_L^* & -s_{L-1}^* & s_{L-2}^*\\ s_{L-1} & s_L & 0\\ 0 & 0 & s_L^* \end{pmatrix} \tag{27a}$$

and

$$\begin{pmatrix} s_1^* & 0 & 0\\ 0 & s_1 & s_2\\ s_3^* & -s_2^* & s_1^*\\ s_2 & s_3 & s_4\\ s_5^* & -s_4^* & s_3^*\\ s_4 & s_5 & s_6\\ \vdots & \vdots & \vdots\\ s_{L-4} & s_{L-3} & s_{L-2}\\ s_{L-1}^* & -s_{L-2}^* & s_{L-3}^*\\ s_{L-2} & s_{L-1} & s_L\\ 0 & -s_L^* & s_{L-1}^*\\ s_L & 0 & 0 \end{pmatrix} \tag{27b}$$

for odd and even L, respectively. It can be seen from (27) that any symbol $\pm s_l$ or $\pm s_l^*$ on the middle column of $X(\mathbf{s})$ belongs to two 2×2 Alamouti codes simultaneously. This is why we use the term "overlapped" in the definition for the novel codes.

Now, let us see the equivalent channel matrix $\mathcal{H}$ corresponding to $\mathcal{O}_{M,L}$ in (26) for odd M. When there is single receive antenna, from (6) and (25), the channel model for $\mathcal{O}_{M,L}$ is

$$\begin{aligned}\bar{\mathbf{y}}&=\sqrt{\frac{\rho}{\mu}}X(\mathbf{s})\mathbf{h}+\bar{\mathbf{w}}\\ &=\sqrt{\frac{\rho}{\mu}}\left(O(\mathbf{s}_o,L,M)+E(\mathbf{s}_e,L,M)\right)\mathbf{h}+\bar{\mathbf{w}}\end{aligned} \tag{28}$$

where $\bar{\mathbf{y}}=(y_1,y_2,\ldots,y_{L+M-1})^t$, $\mathbf{h}=(h_1,h_2,\ldots,h_M)^t$ and $\bar{\mathbf{w}}=(w_1,w_2,\ldots,w_{L+M-1})^t$. To describe the equivalent channel model (3), for odd p, we define matrix $F(\mathbf{v},p,q)$ of q columns as

$$F(\mathbf{v},p,q)=\begin{pmatrix} v_1^* & 0 & \ldots & 0\\ v_2 & v_p & \ldots & 0\\ v_3^* & -v_{p-1}^* & \ldots & 0\\ \vdots & \vdots & \ddots & \vdots\\ v_{p-1} & v_3 & \ldots & v_1^*\\ v_p^* & -v_2^* & \ldots & v_2\\ 0 & v_1 & \ldots & v_3^*\\ \vdots & \vdots & \ddots & \vdots\\ 0 & 0 & \ldots & v_p^* \end{pmatrix} \tag{29a}$$

and

$$\begin{pmatrix} v_1^* & 0 & \ldots & 0 & 0\\ v_2 & v_p & \ldots & 0 & 0\\ v_3^* & -v_{p-1}^* & \ldots & 0 & 0\\ \vdots & \vdots & \ddots & \vdots & \vdots\\ v_p^* & -v_2^* & \ldots & v_1^* & 0\\ 0 & v_1 & \ldots & v_2 & v_p\\ \vdots & \vdots & \ddots & \vdots & \vdots\\ 0 & 0 & \ldots & v_p^* & -v_2^*\\ 0 & 0 & \ldots & 0 & v_1 \end{pmatrix} \tag{29b}$$

for odd and even q, respectively, where $\mathbf{v}=(v_1,v_2,\ldots,v_p)^t$ as before and the number of rows of the matrix is $q+p-1$ for both odd and even q. The definition of $F(\mathbf{v},p,q)$ is like that of $O(\mathbf{v},p,q)$ in (21), but here the vectors $\left(v_1^*,v_2,v_3^*,v_4,\ldots,v_{p-1},v_p^*\right)^t$ and $\left(v_p,-v_{p-1}^*,v_{p-2},-v_{p-3}^*,\ldots,-v_2^*,v_1\right)^t$ alternatively appear in columns. Since each row of $X(\mathbf{s})$ in (25) has its transmitted symbols either all in the form of $\pm s_l$ or all in the form of $\pm s_l^*$, like the transformation from (7) to (8), (28) can be reformulated into the equivalent channel model

$$\mathbf{y}=\sqrt{\frac{\rho}{\mu}}\mathcal{H}\mathbf{s}+\mathbf{w} \tag{30}$$

where the equivalent received signal vector

$$\mathbf{y}=\begin{cases}(y_1^*,y_2,y_3^*,y_4,\ldots,y_{L+M-1}^*)^t,\\ \qquad L \text{ odd}, M \text{ odd}\\ (y_1^*,y_2,y_3^*,y_4,\ldots,y_{L+M-2}^*,y_{L+M-1})^t,\\ \qquad L \text{ even}, M \text{ odd}\end{cases} \tag{31}$$

the equivalent noise vector $\mathbf{w}$ is defined similarly from $\bar{\mathbf{w}}$ and the equivalent channel matrix $\mathcal{H}=F(\mathbf{h},M,L)$ with matrix $F(\cdot,\cdot,\cdot)$ defined in (29). For example, for $\mathcal{O}_{3,L}$ with the codeword matrix $X(\mathbf{s})$ in (27), the corresponding equivalent channel matrix is

$$\mathcal{H}=\begin{pmatrix} h_1^* & 0 & \ldots & 0 & 0\\ h_2 & h_3 & \ldots & 0 & 0\\ h_3^* & -h_2^* & \ldots & 0 & 0\\ 0 & h_1 & \ldots & 0 & 0\\ \vdots & \vdots & \ddots & \vdots & \vdots\\ 0 & 0 & \ldots & -h_2^* & h_1^*\\ 0 & 0 & \ldots & h_1 & h_2\\ 0 & 0 & \ldots & 0 & h_3^* \end{pmatrix}$$

and

$$\begin{pmatrix} h_1^* & 0 & \ldots & 0 & 0\\ h_2 & h_3 & \ldots & 0 & 0\\ h_3^* & -h_2^* & \ldots & 0 & 0\\ 0 & h_1 & \ldots & 0 & 0\\ \vdots & \vdots & \ddots & \vdots & \vdots\\ 0 & 0 & \ldots & h_2 & h_3\\ 0 & 0 & \ldots & h_3^* & -h_2^*\\ 0 & 0 & \ldots & 0 & h_1 \end{pmatrix}$$

for odd and even L, respectively.

Obviously, the $\mathcal{H}$ in (30) satisfies the first part of the criterion (16), i.e., $\|\mathcal{H}\|=\sqrt{L}\|\mathbf{h}\|$, and to show the full diversity

property of $\mathcal{O}_{M,L}$ with ZF or MMSE receiver for odd M and $N = 1$, it suffices for us to show the second part of (16) according to Theorem 1.

Theorem 2: For any given positive integer L and odd M, the matrix $\mathcal{H} = F(\mathbf{h}, M, L)$ satisfies

$$\det(\mathcal{H}^\dagger \mathcal{H}) \geq c\|\mathbf{h}\|^{2L} \tag{32}$$

for any $\mathbf{h}$, where c is a positive constant independent of $\mathbf{h}$, but may depend on M and L.

A proof of Theorem 2 is in Appendix C. Similar to Toeplitz codes, we generally do not have an explicit expression for the constant c in (32) in terms of M and L. However, for the simple case of $M = 3$, i.e., three transmit antennas, we have

$$\det\left(F^\dagger(\mathbf{h}, 3, L)F(\mathbf{h}, 3, L)\right) \geq 3^{-L-(L \bmod 2)}\|\mathbf{h}\|^{2L} \tag{33}$$

for any $\mathbf{h} = (h_1, h_2, h_3)^t$, where $(L \bmod 2)$ denotes the remainder of L divided by 2, and a proof of (33) is in Appendix D.

In general, for N receive antennas, in accordance with the discussion in Section II-A, the equivant channel matrix corresponding to $\mathcal{O}_{M,L}$ for odd M is then

$$\mathcal{H} = (\mathcal{H}_1^t, \mathcal{H}_2^t, \ldots, \mathcal{H}_N^t)^t \tag{34}$$

where $\mathcal{H}_n = F(\mathbf{h}_n, M, L)$ and $\mathbf{h}_n$ is the nth column of the original channel matrix H in (2). From Corollary 1, the $\mathcal{H}$ in (34) still satisfies (16) and thus, $\mathcal{O}_{M,L}$ with odd M achieves full diversity with ZF or MMSE receiver for any number of receive antennas.

B. Overlapped Alamouti Codes for Even Transmit Antennas

The proposed overlapped Alamouti codes for even transmit antennas M, which is still denoted by $\mathcal{O}_{M,L}$, can be easily obtained from the preceding construction of $\mathcal{O}_{M+1,L}$ for odd transmit antennas $M + 1$, by eliminating either the first or the last column of the codeword matrix $X(\mathbf{s}) = O(\mathbf{s}_o, L, M+1) + E(\mathbf{s}_e, L, M+1)$ of $\mathcal{O}_{M+1,L}$ in (25). Note that eliminating any other column of $X(\mathbf{s})$ to obtain the codeword matrix of $\mathcal{O}_{M,L}$ is infeasible because that will destroy the overlapped Alamouti structure of the original matrix. It is not hard to check that the symbol rate of the resulting $\mathcal{O}_{M,L}$ by this method is

$$R_{\mathcal{O}_{M,L}} = \begin{cases} \frac{L}{L+M-1}, & L \text{ odd}, M \text{ even} \\ \frac{L}{L+M}, & L \text{ even}, M \text{ even} \end{cases}$$

if we delete the last column of the codeword matrix of $\mathcal{O}_{M+1,L}$, or alternatively

$$R_{\mathcal{O}_{M,L}} = \begin{cases} \frac{L}{L+M-1}, & L \text{ odd}, M \text{ even} \\ \frac{L}{L+M-2}, & L \text{ even}, M \text{ even} \end{cases}$$

if we instead delete the first column of the codeword matrix of $\mathcal{O}_{M+1,L}$. Therefore, we adopt the latter, i.e., the first column elimination method, to generate the codeword matrix of $\mathcal{O}_{M,L}$ for the higher symbol rate for even L case.

Specifically, to formally define the codeword matrix of $\mathcal{O}_{M,L}$ for even M, we first supplement the definition of $\mathbf{s}_o$ and $\mathbf{s}_e$ in (23) and (24), respectively, for even M as follows:

$$\mathbf{s}_o = \begin{cases} (s_1, 0, s_3, 0, \ldots, 0, s_L)^t, & L \text{ odd}, M \text{ even} \\ (s_1, 0, s_3, 0, \ldots, s_{L-1})^t, & L \text{ even}, M \text{ even} \end{cases} \tag{35}$$

and

$$\mathbf{s}_e = \begin{cases} (s_2, 0, s_4, \ldots, s_{L-1}, 0, 0)^t, & L \text{ odd}, M \text{ even} \\ (s_2, 0, s_4, \ldots, 0, s_L)^t, & L \text{ even}, M \text{ even} \end{cases} \tag{36}$$

which, as before, keep the components of $\mathbf{s}$ with odd and even indices, respectively. However, the length of $\mathbf{s}_o$ and $\mathbf{s}_e$ is now L if L is odd and $L - 1$ if L is even. Then, by eliminating the first column of the codeword matrix of $\mathcal{O}_{M+1,L}$, we have the codeword matrix of $\mathcal{O}_{M,L}$ for even M defined as (37) shown at the bottom of the page where $\mathbf{s}_o$ and $\mathbf{s}_e$ are defined in (35) and (36), respectively, and matrices $O(\cdot,\cdot,\cdot)$ and $E(\cdot,\cdot,\cdot)$ are defined in (21) and (22), respectively. Correspondingly, for even M

$$\mathcal{O}_{M,L} = \{X(\mathbf{s}) \text{ in } (37), \quad \mathbf{s} = (s_1, s_2, \ldots, s_L)^t \in \mathcal{C}^L\}. \tag{38}$$

As simple examples, we give the codeword matrices of $\mathcal{O}_{M,L}$ for $M = 2$ and $M = 4$ below. When $M = 2$, the codeword matrix $X(\mathbf{s})$ of $\mathcal{O}_{2,L}$ is just the one obtained by eliminating the first column of the matrix in (27), resulting in

$$X(\mathbf{s}) = \begin{pmatrix} s_1 & s_2 \\ -s_2^* & s_1^* \\ s_3 & s_4 \\ -s_4^* & s_3^* \\ \vdots & \vdots \\ s_{L-2} & s_{L-1} \\ -s_{L-1}^* & s_{L-2}^* \\ s_L & 0 \\ 0 & s_L^* \end{pmatrix} \text{ and } \begin{pmatrix} s_1 & s_2 \\ -s_2^* & s_1^* \\ s_3 & s_4 \\ -s_4^* & s_3^* \\ \vdots & \vdots \\ s_{L-3} & s_{L-2} \\ -s_{L-2}^* & s_{L-3}^* \\ s_{L-1} & s_L \\ -s_L^* & s_{L-1}^* \end{pmatrix} \tag{39}$$

for odd and even L, respectively. Not surprisingly, $\mathcal{O}_{2,L}$ is just $\frac{L}{2}$ concatenated Alamouti codes for even L, which results from the overlapped Alamouti structure in $\mathcal{O}_{3,L}$. So, the proposed overlapped Alamouti codes cover the classical Alamouti code as

$$X(\mathbf{s}) = \begin{cases} O(\mathbf{s}_o^*, L, M) + E(\mathbf{s}_e, L, M), & L \text{ odd}, M \text{ even} \\ O(\mathbf{s}_o^*, L-1, M) + E(\mathbf{s}_e, L-1, M), & L \text{ even}, M \text{ even} \end{cases} \tag{37}$$

a special case when $M = L = 2$. When $M = 4$, the codeword matrix of $\mathcal{O}_{4,L}$ is

$$X(\mathbf{s}) = \begin{pmatrix} s_1 & 0 & 0 & s_2 \\ 0 & s_1^* & -s_2^* & 0 \\ s_3 & s_2 & s_1 & s_4 \\ -s_2^* & s_3^* & -s_4^* & s_1^* \\ s_5 & s_4 & s_3 & s_6 \\ \vdots & \vdots & \vdots & \vdots \\ -s_{L-3}^* & s_{L-2}^* & -s_{L-1}^* & s_{L-4}^* \\ s_L & s_{L-1} & s_{L-2} & 0 \\ -s_{L-1}^* & s_L^* & 0 & s_{L-2}^* \\ 0 & 0 & s_L & 0 \\ 0 & 0 & 0 & s_L^* \end{pmatrix} \tag{40a}$$

and

$$\begin{pmatrix} s_1 & 0 & 0 & s_2 \\ 0 & s_1^* & -s_2^* & 0 \\ s_3 & s_2 & s_1 & s_4 \\ -s_2^* & s_3^* & -s_4^* & s_1^* \\ s_5 & s_4 & s_3 & s_6 \\ \vdots & \vdots & \vdots & \vdots \\ -s_{L-4}^* & s_{L-3}^* & -s_{L-2}^* & s_{L-5}^* \\ s_{L-1} & s_{L-2} & s_{L-3} & s_L \\ -s_{L-2}^* & s_{L-1}^* & -s_L^* & s_{L-3}^* \\ 0 & s_L & s_{L-1} & 0 \\ -s_L^* & 0 & 0 & s_{L-1}^* \end{pmatrix} \tag{40b}$$

for odd and even L, respectively. As in (27), the overlapped Alamouti structure can be easily observed in (40), i.e., each information symbol $\pm s_l$ or $\pm s_l^*$ belongs to two 2×2 Alamouti codes simultaneously, except for those on the most left and the most right columns.

Let us now describe the equivalent channel model corresponding to $\mathcal{O}_{M,L}$ for even M. For single receive antenna, the original channel model is (6) with $X(\mathbf{s})$ given in (37) and the equivalent channel model also has the form of (30), where, however, the length of $\bar{\mathbf{y}}$, $\bar{\mathbf{w}}$, $\mathbf{y}$ and $\mathbf{w}$ is $L + M - 1$ for odd L and $L + M - 2$ for even L and furthermore, similar to the definition of $\mathbf{y}$ in (31), the equivalent received signal vector $\mathbf{y}$ is now

$$\mathbf{y} = \begin{cases} \left(y_1, y_2^*, y_3, y_4^*, \ldots, y_{L+M-1}^*\right)^t, & L \text{ odd}, M \text{ even} \\ \left(y_1, y_2^*, y_3, y_4^*, \ldots, y_{L+M-2}^*\right)^t, & L \text{ even}, M \text{ even} \end{cases}$$

and $\mathbf{w}$ is generated similarly from $\bar{\mathbf{w}}$ by conjugating the components with even indices in $\bar{\mathbf{w}}$.

Since the first column of the codeword matrix corresponds to the first component of the channel matrix (vector) in the model (6) for single receive antenna, the equivalent channel matrix for $\mathcal{O}_{M,L}$ with even M is easily obtained by setting the first component of the channel matrix (vector) to be 0 in the equivalent channel matrix for $\mathcal{O}_{M+1,L}$, which has been characterized by the matrix $F(\mathbf{v}, p, q)$ in (29). With this observation, to characterize the equivalent channel matrix corresponding to $\mathcal{O}_{M,L}$ for even M, we supplement the definition of the matrix $F(\mathbf{v}, p, q)$ of q columns for even p as

$$F(\mathbf{v}, p, q) = \begin{pmatrix} v_1 & v_p & 0 & 0 & \ldots & 0 \\ v_2^* & -v_{p-1}^* & 0 & 0 & \ldots & 0 \\ v_3 & v_{p-2} & v_1 & v_p & \ldots & 0 \\ \vdots & \vdots & \vdots & \vdots & \ddots & \vdots \\ v_p^* & -v_1^* & v_{p-2}^* & -v_3^* & \ldots & v_1 \\ 0 & 0 & v_{p-1} & v_2 & \ldots & v_2^* \\ 0 & 0 & v_p^* & -v_1^* & \ldots & v_3 \\ \vdots & 0 & 0 & \vdots & \ddots & \vdots \\ 0 & 0 & 0 & 0 & \ldots & v_p^* \end{pmatrix} \tag{41a}$$

and

$$\begin{pmatrix} v_1 & v_p & \ldots & 0 & 0 \\ v_2^* & -v_{p-1}^* & \ldots & 0 & 0 \\ \vdots & \vdots & \ddots & \vdots & \vdots \\ v_{p-2}^* & -v_3^* & \ldots & 0 & 0 \\ v_{p-1} & v_2 & \ldots & v_1 & v_p \\ v_p^* & -v_1^* & \ldots & v_2^* & -v_{p-1}^* \\ \vdots & \vdots & \ddots & \vdots & \vdots \\ 0 & 0 & \ldots & v_{p-1} & v_2 \\ 0 & 0 & \ldots & v_p^* & -v_1^* \end{pmatrix} \tag{41b}$$

for odd and even q, respectively, where $\mathbf{v} = (v_1, v_2, \ldots, v_p)^t$ as before. Note that the number of rows of $F(\mathbf{v}, p, q)$ in (41) is $q + p - 1$ for odd q and $q + p - 2$ for even q. Then, when $N = 1$, the equivalent channel matrix for $\mathcal{O}_{M,L}$ with even M is still $\mathcal{H} = F(\mathbf{h}, M, L)$ with matrix $F(\cdot, \cdot, \cdot)$ defined in (41), which obviously satisfies the first part of the criterion (16), i.e., $\mathcal{H} = \sqrt{L}\|\mathbf{h}\|$, in Theorem 1.

The second part of (16) for $\mathcal{H} = F(\mathbf{h}, M, L)$ with even M can be easily shown by utilizing the preceding result in Theorem 2. Specifically, for any vector $\mathbf{h} = (h_1, h_2, \ldots, h_M)^t$ of length M, we have from the definitions of $F(\mathbf{v}, p, q)$ in (29) and (41) that

$$\begin{aligned} &\det\left(F^\dagger(\mathbf{h}, M, L)F(\mathbf{h}, M, L)\right) \\ &\qquad = \det\left(F^\dagger(\mathbf{h}', M+1, L)F(\mathbf{h}', M+1, L)\right) \end{aligned}$$

where $\mathbf{h}' = (0, h_1, h_2, \ldots, h_M)^t$. Because $\mathbf{h}'$ is just a special vector of length $M + 1$ with the first constant component 0, we know according to Theorem 2 that

$$\begin{aligned} &\det\left(F^\dagger(\mathbf{h}', M+1, L)F(\mathbf{h}', M+1, L)\right) \\ &\quad \geq c\|\mathbf{h}'\|^{2L} \\ &\quad = c\|\mathbf{h}\|^{2L} \end{aligned}$$

where c is a positive constant independent of $\mathbf{h}'$ and thus $\mathbf{h}$. Therefore, from Theorem 1, $\mathcal{O}_{M,L}$ in (38) for even M achieves full diversity with ZF or MMSE receiver for single receive antenna. Similar to the proof of (33) for three transmit antennas in Appendix D, for $M = 4$, i.e., four transmit antennas, we have

$$\det\left(F^\dagger(\mathbf{h}, 4, L)F(\mathbf{h}, 4, L)\right) \geq 4^{-L-(L \bmod 2)}\|\mathbf{h}\|^{2L}$$

for any $\mathbf{h} = (h_1, h_2, h_3, h_4)^t$ by using the result in (20).

For multiple receive antennas, the equivalent channel matrix for $\mathcal{O}_{M,L}$ with even M is still the $\mathcal{H}$ in (34), where the matrix

$F(\cdot,\cdot,\cdot)$ is instead defined in (41) as M is even, and from Corollary 1, $\mathcal{O}_{M,L}$ has full diversity when ZF or MMSE receiver is used for any number of transmit antennas.

We present the following theorem that summarizes the main results for the overlapped Alamouti code $\mathcal{O}_{M,L}$ constructed in this section for both odd and even M.

Theorem 3: For any given positive integers L, M and N, the $\mathcal{H}$ in (34) with $\mathcal{H}_n = F(\mathbf{h}_n, M, L)$ is an equivalent channel matrix corresponding to the overlapped Alamouti code $\mathcal{O}_{M,L}$ defined in (26) and (38), where $F(\mathbf{h}_n, M, L)$ is defined in (29) and (41) for odd and even M, respectively, and $\mathbf{h}_n$ is the nth column of the original channel matrix H in (2). This $\mathcal{H}$ satisfies the criterion (16) in Theorem 1 and hence overlapped Alamouti codes achieve full diversity with ZF or MMSE receiver.

C. Equivalent Overlapped Alamouti Codes

The structure of the overlapped Alamouti codes proposed in Sections III-A and B is not unique, just as the Alamouti code that has several different but equivalent forms. For instance, in Section III-B, we have constructed the codeword matrix of $\mathcal{O}_{M,L}$ for even M by eliminating the first column of the codeword matrix of $\mathcal{O}_{M+1,L}$. Alternatively, this method can also be used to construct $\mathcal{O}_{M,L}$ for odd M. Specifically, if we already have the construction of $\mathcal{O}_{M+1,L}$ in (38) for odd M, by eliminating the last column of its codeword matrix $X(\mathbf{s})$ in (37), we then obtain the codeword matrix of an overlapped Alamouti code that is equivalent to $\mathcal{O}_{M,L}$ in (26) as

$$X(\mathbf{s}) = O(\mathbf{s}_o^*, L, M) + E(-\mathbf{s}_e^*, L, M)$$

where $\mathbf{s}_o$ and $\mathbf{s}_e$ are defined in (23) and (24), respectively, for odd M.

Some other equivalent constructions (structures) of overlapped Alamouti codes are also available. One equivalence is from the different equivalent structures of Alamouti code. For example,

$$\begin{pmatrix} s_1 & s_2 \\ -s_2^* & s_1^* \end{pmatrix} \text{ and } \begin{pmatrix} s_1^* & -s_2^* \\ s_2 & s_1 \end{pmatrix}$$

are the codeword matrices of two equivalent Alamouti codes. In terms of this equivalence, if the codeword matrix $X(\mathbf{s})$ of an STBC has any one of the forms in (42) shown at the bottom of the page, this STBC is an equivalent overlapped Alamouti code, where $\mathbf{s}_o$ and $\mathbf{s}_e$ are defined in (23) and (24) or (35) and (36) for odd and even M, respectively. This equivalence affected in the corresponding equivalent channel matrix $\mathcal{H}$ in (34) is to conjugate $\mathcal{H}_n$ and/or change the signs of the odd and/or even columns of $\mathcal{H}_n$, $n = 1, 2, \ldots, N$.

Besides the above equivalence, another equivalence is up to the permutation of the columns of the codeword matrices of overlapped Alamouti codes. At first glance, this operation would "destroy" the overlapped Alamouti structure of the original code. However, the orthogonality among the columns is fully kept despite of the permutation, which essentially determines the performance of the code with linear receivers. Moreover, by identifying Alamouti codes on two columns that may not be adjacent, we can still recognize the overlapped Alamouti structure in the resulting code. Such a column permutation on the codeword matrix results in the corresponding row permutation of the original channel matrix H and also the corresponding permutation of the components $\{h_{m,n}\}_{m=1}^{M}$ in the submatrix $\mathcal{H}_n$, $n = 1, 2, \ldots, N$, of the equivalent channel matrix $\mathcal{H}$ in (34).

D. Some Properties of Overlapped Alamouti Codes

Our proposed overlapped Alamouti codes have some good properties that will be investigated and described in this subsection, and their performance comparison with some other STBC is to be carried out in Section IV. We now make the following remarks for overlapped Alamouti codes and the main counterparts in the comparison are OSTBC and Toeplitz codes.

1) *Symbol rate*. Overlapped Alamouti codes have symbol rates

$$R_{\mathcal{O}_{M,L}} = \begin{cases} \frac{L}{L+M-2}, & L \,\&\, M \text{ even} \\ \frac{L}{L+M-1}, & \text{otherwise} \end{cases} \tag{43}$$

which are slightly higher than $R_{\mathcal{T}_{M,L}}$ in (12) for Toeplitz codes when both M and L are even, and can approach 1 as L goes to infinity for a fixed M. Also, $R_{\mathcal{O}_{M,L}}$ is strictly less than 1 unless $M = 2$ and L is even, i.e., $R_{\mathcal{O}_{M,L}} = 1$ if and only if $\mathcal{O}_{M,L}$ is equivalent to $L/2$ concatenated Alamouti codes. So, under the criterion in Theorem 1, overlapped Alamouti codes and Toeplitz codes are asymptotically optimal in terms of symbol rates according to Corollary 2. However, for OSTBC, the symbol rates are upper bounded by $3/4$ for more than two transmit antennas and furthermore, a tight upper bound was conjectured to be $(k+1)/(2k)$ for $2k$ or $2k-1$ transmit antennas in [7]. Hence, overlapped Alamouti codes have more flexible and, generally, higher rates than OSTBC.

2) *Orthogonality*. If we say the first column and the last column of a matrix are adjacent in a cyclic way, for $\mathcal{O}_{M,L}$ in (26) and (38), each column in its codeword matrix must be orthogonal to its two adjacent columns except that when M is odd, the first and the Mth columns are only orthogonal to the second and the $(M-1)$th columns, respectively. Nevertheless, for Toeplitz codes, no orthogonality exists in their codeword matrices.

Observing the corresponding equivalent channel matrices $\mathcal{H}$ is another way to evaluate the orthogonality of the codes. For OSTBC, they have perfect orthogonality and the corresponding $\mathcal{H}$ is a scaled unitary matrix. For overlapped Alamouti codes, on the other hand, all the odd columns of

$$\begin{cases} O(\pm\mathbf{s}_o, L, M) + E(\pm\mathbf{s}_e, L, M) \text{ or } O(\pm\mathbf{s}_o^*, L, M) + E(\pm\mathbf{s}_e^*, L, M), & M \text{ odd} \\ O(\pm\mathbf{s}_o^*, L, M) + E(\pm\mathbf{s}_e, L, M) \text{ or } O(\pm\mathbf{s}_o, L, M) + E(\pm\mathbf{s}_e^*, L, M), & L \text{ odd}, M \text{ even} \\ O(\pm\mathbf{s}_o^*, L-1, M) + E(\pm\mathbf{s}_e, L-1, M) \text{ or } O(\pm\mathbf{s}_o, L-1, M) + E(\pm\mathbf{s}_e^*, L-1, M), & L \text{ even}, M \text{ even} \end{cases} \tag{42}$$

the equivalent channel matrix $\mathcal{H}$ in (34) are orthogonal to all its even columns as we can see from the definition of $F(\mathbf{v}, p, q)$ in (29) and (41), which efficiently reduces the interference between the transmitted information symbols because the symbols s_l with odd indices are then independent of those with even indices. Equation (54) in the proof of Theorem 2 in Appendix C is another efficient method to observe this orthogonality, where for single receive antenna, matrix $\mathcal{H}^\dagger\mathcal{H}$ has been decomposed into

$$\mathcal{H}^\dagger\mathcal{H} = \mathcal{H}_o^\dagger\mathcal{H}_o + \mathcal{H}_e^\dagger\mathcal{H}_e \tag{44}$$

with $\mathcal{H}_o$ resulted from $\mathcal{H}$ by setting the components of the channel matrix (vector) $\mathbf{h}$ with even indices to be 0 and $\mathcal{H}_e = \mathcal{H} - \mathcal{H}_o$. Finally, for Toeplitz codes, there is no orthogonality in their corresponding equivalent channel matrices.

To illustrate this property from an intuitive point of view, in Fig. 1, we compare the average condition numbers[3] of the matrices $\mathcal{H}^\dagger\mathcal{H}$ ($\mathcal{H}$ is the equivalent channel matrix in (3)) for overlapped Alamouti codes and Toeplitz codes that dominate the performance of ZF or MMSE receiver. It can be observed from Fig. 1 that the matrix for overlapped Alamouti codes is much less singular than that for Toeplitz codes and furthermore, unlike Toeplitz codes, the condition number for overlapped Alamouti codes is quite stable, i.e., it has no significant increase as L increases. Based on this observation, we may expect the performance of Toeplitz codes degrades rapidly as L becomes large for a fixed number of transmit antennas, while for overlapped Alamouti codes, this performance loss should be much smaller.

3) *Block length*. First, compared with Toeplitz codes, the block lengths of overlapped Alamouti codes are slightly shorter when both M and L are even. For OSTBC, when $M = 2$, Alamouti code has the highest rate 1 and overlapped Alamouti codes cover it as a special case. For more than two transmit antennas, to achieve the conjectured maximum symbol rate of $(k+1)/(2k)$ for $2k$ or $2k-1$ transmit antennas for OSTBC [7], overlapped Alamouti codes need to have block length $4k$. When $M > 4$, this length is much smaller than the block lengths of the existing constructions for OSTBC with the conjectured maximum rates in the literature [8]–[10].
4) *Decoding complexity*. In comparison with OSTBC that have simple ML decoding algorithm, the decoding complexities of Toeplitz codes and overlapped Alamouti codes are higher, which mainly results from the matrix inverse operation $(\mathcal{H}^\dagger\mathcal{H})^{-1}$ and $(\frac{\rho}{\mu}\mathcal{H}^\dagger\mathcal{H} + I_L)^{-1}$ for ZF receiver (14) and MMSE receiver (15), respectively. However, for overlapped Alamouti codes, according to (44) as well as (55) and (56) in Appendix C, we have

$$\begin{aligned}\mathcal{H}^\dagger\mathcal{H} &= \left(T_o^\dagger T_o + T_e^\dagger T_e\right) \otimes I_2 \\ \Rightarrow (\mathcal{H}^\dagger\mathcal{H})^{-1} &= \left(T_o^\dagger T_o + T_e^\dagger T_e\right)^{-1} \otimes I_2\end{aligned} \tag{45}$$

when L is even, where T_o and T_e are two Toeplitz matrices with $L/2$ columns and $\otimes$ denotes the Kronecker product between two matrices. From (45), to obtain $(\mathcal{H}^\dagger\mathcal{H})^{-1}$, it suffices for us to calculate the inverse of $T_o^\dagger T_o + T_e^\dagger T_e$, which is only of half dimension of $\mathcal{H}^\dagger\mathcal{H}$. When L is odd, on the other hand, from the results on the inverse of a partitioned matrix [53, p. 29], the inverse of the matrix $\mathcal{H}^\dagger\mathcal{H}$ for some $\mathcal{O}_{M,L}$ can be easily derived from its counterpart for $\mathcal{O}_{M,L-1}$ with a slightly more matrix multiplication operations, while a simplified calculation for the latter already exists in (45). So, benefitting from this property, the decoding complexity of overlapped Alamouti codes becomes much smaller than that of Toeplitz codes for ZF receiver. With a similar derivation, a simplified calculation of $(\frac{\rho}{\mu}\mathcal{H}^\dagger\mathcal{H} + I_L)^{-1}$ for MMSE receiver also exists for overlapped Alamouti codes.

5) *Diversity-Multiplexing Tradeoff*. It has been shown in [20], [21] that in an independent MISO flat fading channel, Toeplitz codes can approach the diversity-multiplexing tradeoff [45] with ZF or MMSE receiver for square QAM constellation. Since our overlapped Alamouti codes have the same diversity as and slightly higher symbol rates than Toeplitz codes, they can also approach the diversity-multiplexing tradeoff in the same situation.

In summary, overlapped Alamouti codes are consistently superior to Toeplitz codes in all the above aspects in consideration. Compared with OSTBC, overlapped Alamouti codes have symbol rate and block length advantages. Therefore, althoughoverlapped Alamouti codes can not outperform OSTBC in the case when their symbol rates are the same due to the perfect orthogonality of the latter, the higher available rates of overlapped Alamouti codes can compensate the drawback of orthogonality and may lead to performance gains over OSTBC. For example, an OSTBC that uses 16-QAM constellation may be outperformed by an overlapped Alamouti code, which uses 4-QAM constellation, with a higher symbol rate but the same throughput, and furthermore, the overlapped Alamouti code generally has a smaller block length than the OSTBC when the number of transmit antennas is not small. The above observation will be verified from the simulation results in Section IV.

IV. Simulation Results

We next present some simulation results to compare the performance of overlapped Alamouti codes with some known STBC. In all the simulations, the channel model follows that described in Section II-A except that, for simplicity, the covariance matrix Σ for the original channel matrix H is assumed to be an identity matrix, i.e., the channel coefficients $h_{m,n}$ are independently and identically $\mathcal{CN}(0,1)$ distributed. Furthermore, the mapping from information bits to symbols in all the constellations used in the simulations are Gray mapping. To investigate the performance of overlapped Alamouti codes when they are concatenated with a forward error correcting code as what is usually done in a practical system, we use a rate

[3]In this paper, the condition number of a matrix means the ratio of its largest singular value to its smallest singular value.

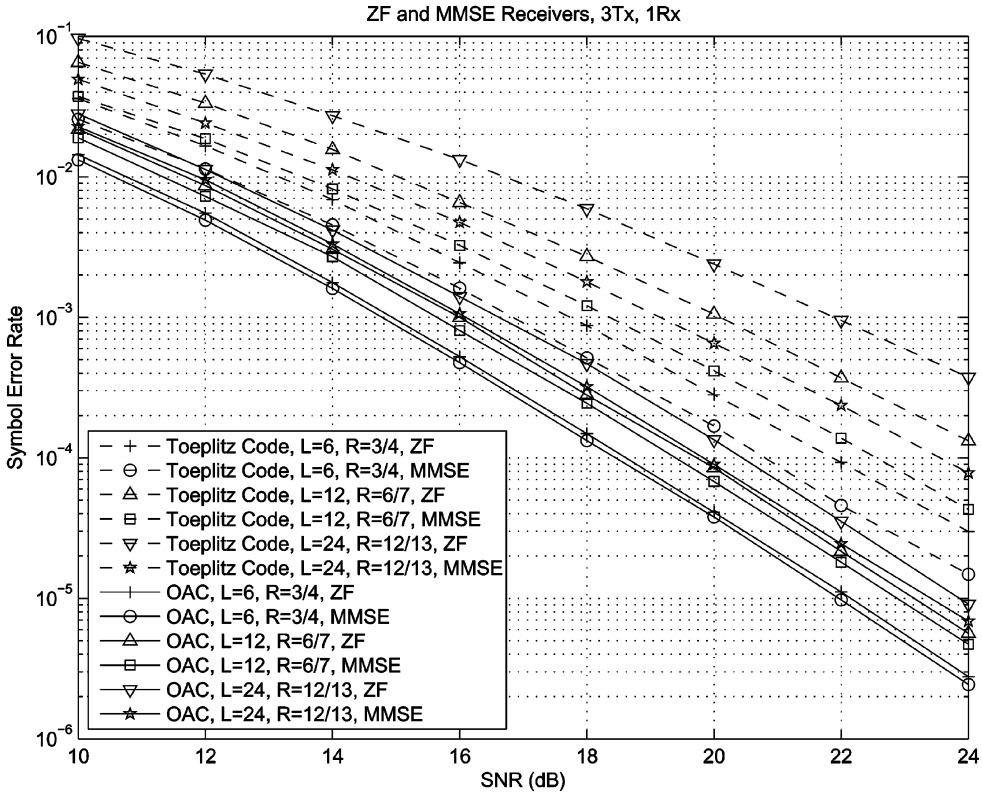

(a)

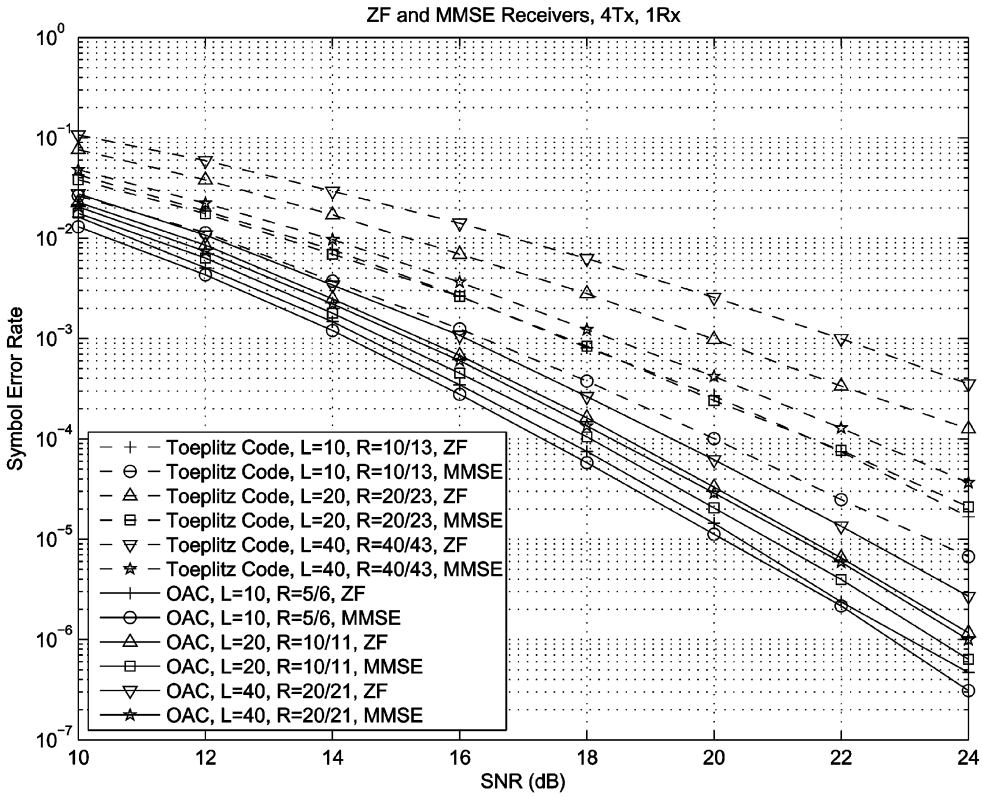

(b)

Fig. 2. Comparison of the performances for overlapped Alamouti codes and Toeplitz codes with linear receivers: (a) three transmit and one receive antennas (4-QAM) and (b) four transmit and one receive antennas (4-QAM).

$1/2$ convolutional code with generator polynomials $(171, 133)$ (in octal numbers) and constraint length 7 as an outer code that has been adopted in IEEE 802.16d WiMAX standard. This outer convolutional code is decoded by Viterbi algorithm with soft in

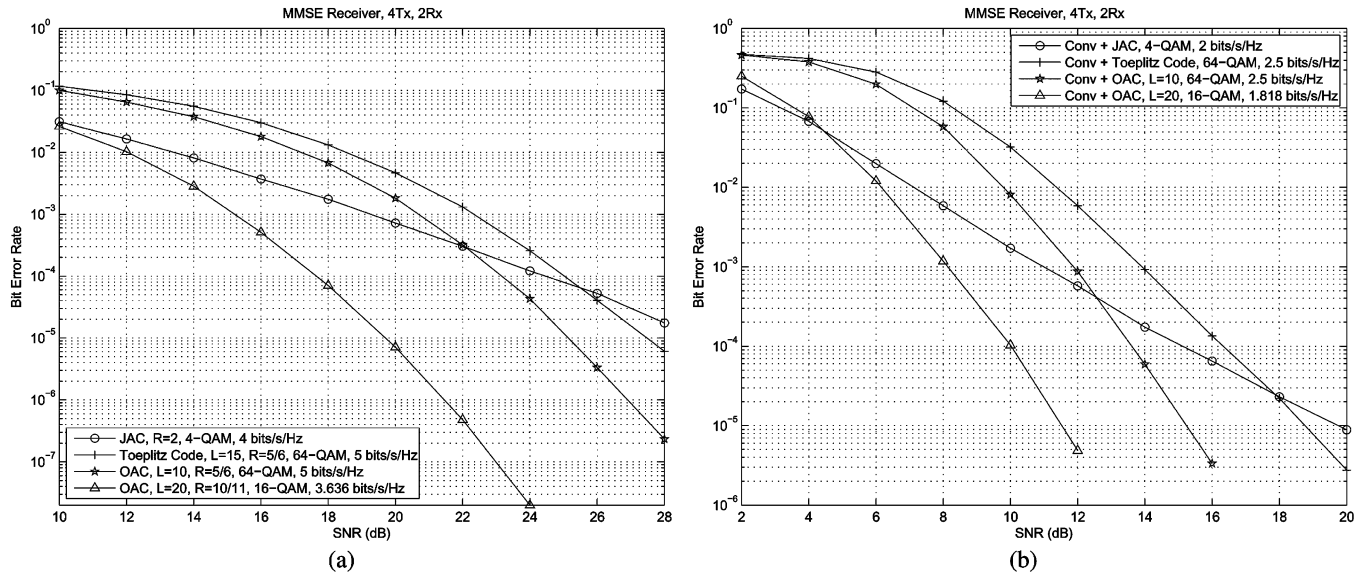

Fig. 3. Comparison of the performances for overlapped Alamouti codes, Toeplitz codes and JAC in (46) with MMSE receiver for four transmit and two receive antennas: (a) without outer convolutional codes and (b) with outer convolutional codes.

puts. In all the simulation figures, the terms "OAC" and "Conv" stand for overlapped Alamouti codes and convolutional codes, respectively. Note that when $M = 2$, i.e., two transmit antennas, overlapped Alamouti codes are equivalent to Alamouti code for even L and hence we do not investigate their performance.

A. Overlapped Alamouti Codes Versus Toeplitz Codes: $M = 3$ or 4, $N = 1$

In Fig. 2, we compare the symbol error rate (SER) performances of overlapped Alamouti codes and Toeplitz codes in an MIMO system with three or four transmit antennas and one receive antenna. 4-QAM constellation is used. It is easy to see that our overlapped Alamouti codes significantly outperform Toeplitz codes for as least 2.5 dB (when L is small and MMSE receiver is used) at SER equal to 10^{-4}. As we may expect from Fig. 1, the performance loss for overlapped Alamouti codes as L increases, i.e., symbol rate improves, is much smaller than that for Toeplitz codes. For example, we can see from both figures that for ZF receiver at SER equal to 10^{-3}, the SNR loss for overlapped Alamouti codes is less than 1 dB as L becomes twice larger and, however, Toeplitz codes have at least 2 dB loss in the same scenario. Furthermore, the performance improvement of MMSE receiver over ZF receiver for overlapped Alamouti codes is not as significant as that for Toeplitz codes, and this is because the orthogonality of the equivalent channel matrix for overlapped Alamouti codes is much better than that for Toeplitz codes as we have discussed in Section III-D.

B. Overlapped Alamouti Codes Versus Juxtaposed Alamouti Code: $M = 4$, $N = 2$

Recently, an STBC with the form of two juxtaposed Alamouti codes is proposed in 3GPP, which is transmitted from 4 antennas and has symbol rate 2. We call this code as juxtaposed Alamouti code, JAC for short. Specifically, the codeword matrix of JAC is

$$X(\mathbf{s}) = \begin{pmatrix} s_1 & s_2 & s_3 & s_4 \\ -s_2^* & s_1^* & -s_4^* & s_3^* \end{pmatrix}. \tag{46}$$

It is obvious that JAC only has diversity order 2, rather than the full diversity order 4, with ML receiver and hence can not achieve full diversity with linear receivers. In Fig. 3(a), the performances of JAC, overlapped Alamouti codes and Toeplitz codes are compared, where the number of receive antennas is two so that linear receivers are feasible for JAC. Since 4-QAM constellation is used for JAC (throughput is 4 bits/s/Hz), to have a comparable throughput, we use 16-QAM constellation for one overlapped Alamouti code with $L = 20$ (throughput is 3.636 bits/s/Hz) and 64-QAM constellation for the other one with $L = 10$ (throughput is 5 bits/s/Hz). The Toeplitz code uses $L = 15$ so that it has the same symbol rate as the overlapped Alamouti code with $L = 10$. We can observe from Fig. 3(a) that the overlapped Alamouti codes not only outperform the Toeplitz code but also have significant diversity gains over JAC, while the latter has much shorter block length. For the overlapped Alamouti code that has 25% more throughput than JAC, it outperforms JAC for the bit error rate (BER) levels we are interested in in practice and for the other overlapped Alamouti code with a slightly smaller throughput, its performance is significantly and consistently superior to that of JAC.

In Fig. 3(b), the same performance comparison as that in Fig. 3(a) is carried out when the codes are concatenated with an outer convolutional code. To have a fair comparison, the MIMO channel changes independently per 18 blocks (36 channel uses), two blocks (36 channel uses), three blocks (36 channel uses), and two blocks (44 channel uses) for JAC, the Toeplitz code, the overlapped Alamouti code with $L = 10$ and the other overlapped Alamouti code with $L = 20$, respectively. The length of the input information bit sequence to the convolutional code is 360 bits that is a common multiple of the numbers of bits per block for the four codes. Furthermore, all the codes are MMSE decoded to extract soft outputs. As we can observe in Fig. 3(b), the convolutional code has contributed at least 7dB reduction in SNR at BER equal to 10^{-4}, compared with the performances of the codes in Fig. 3(a), while the relative trends among their performance curves are still kept. As a result, the overlapped

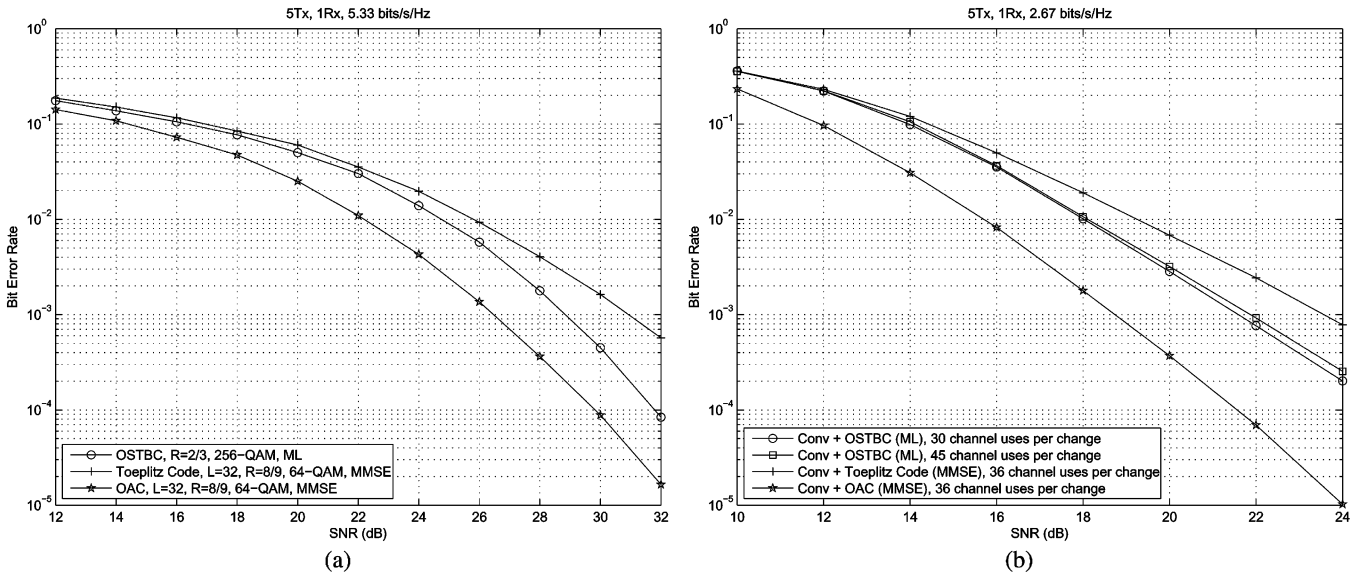

Fig. 4. Comparison of the performances of an overlapped Alamouti code, a Toeplitz code and an OSTBC with the same throughput for five transmit and one receive antennas: (a) without outer convolutional codes and (b) with outer convolutional codes.

Alamouti codes also outperform the Toeplitz code and JAC when they are concatenated with outer convolutional codes.

C. Overlapped Alamouti Codes Versus OSTBC: $M = 5$ or 8, $N = 1$

We have analyzed in Section III-D that overlapped Alamouti codes can have higher rates than OSTBC for $M > 2$, which may lead to performance gains. To illustrate this, in Fig. 4(a), we compare the performances of an overlapped Alamouti code, a Toeplitz code and an OSTBC in an MIMO system with five transmit and one receive antennas. The highest known rate of OSTBC for five transmit antennas is $2/3$ in the literature and here we adopt the one in [10, p. 4345] with block length 15. We choose $L = 32$ for the overlapped Alamouti code and the Toeplitz code, both of which use 64-QAM constellation, and the OSTBC uses 256-QAM constellation. So, all the three codes have the same throughput of 5.33 bits/s/Hz. It can be seen from Fig. 4(a) that the overlapped Alamouti code has the best performance among the three codes, consistently outperforming the OSTBC in the SNR range of interest and having about 2 dB coding gain over the OSTBC at the BER equal to 10^{-4}, and the Toeplitz code performs the worst, where the OSTBC is ML decoded and the overlapped Alamouti code and the Toeplitz code are MMSE decoded.

Similar to Fig. 3(b), a performance comparison of the codes in Fig. 4(a) when they are concatenated with an outer convolutional code is presented in Fig. 4(b), where the Toeplitz code and the overlapped Alamouti code use MMSE receiver to extract soft outputs and the OSTBC uses (9) to obtain soft outputs. The block number per channel change is two (36 channel uses) for both the Toeplitz code and the overlapped Alamouti code. Since 36 is not an integer multiple of the block length 15 of the OSTBC, we provide two simulation curves for the OSTBC, one for two blocks (30 channel uses) per channel change and the other for three blocks (45 channel uses) per channel change. The length of the input information sequence to the convolutional code is 480 bits. As we can expect from Fig. 4(a), while the concatenated outer code has significantly improved the performances for all the three codes, the overlapped Alamouti code still outperforms the others.

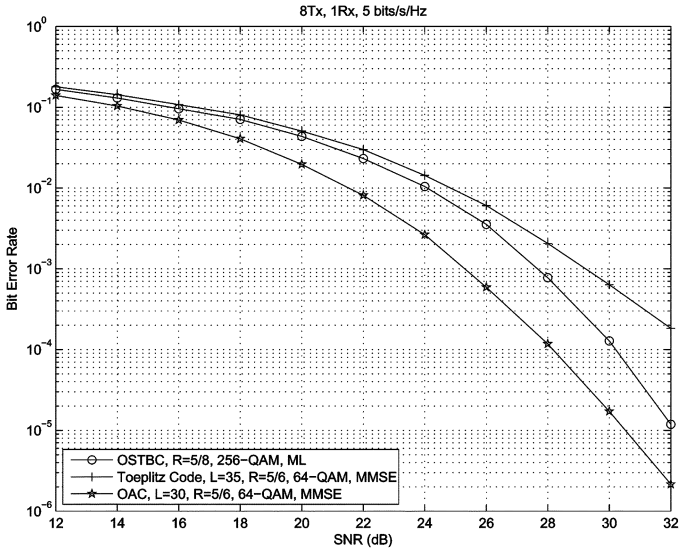

Fig. 5. Comparison of the performances of an overlapped Alamouti code, a Toeplitz code and an OSTBC with the same throughput of 5 bits/s/Hz for eight transmit and one receive antennas.

Similar performance improvements of overlapped Alamouti codes over OSTBC as that in Fig. 4(a) have been also observed for more than five transmit antennas, where with the same throughput, overlapped Alamouti codes have shorter block lengths than OSTBC. As an example, in Fig. 5, the performances of an overlapped Alamouti code with $L = 30$, a Toeplitz code with $L = 35$ and an OSTBC are compared for eight transmit and one receive antennas, where the OSTBC is the one in [10, p. 4346] that has the highest known symbol rate

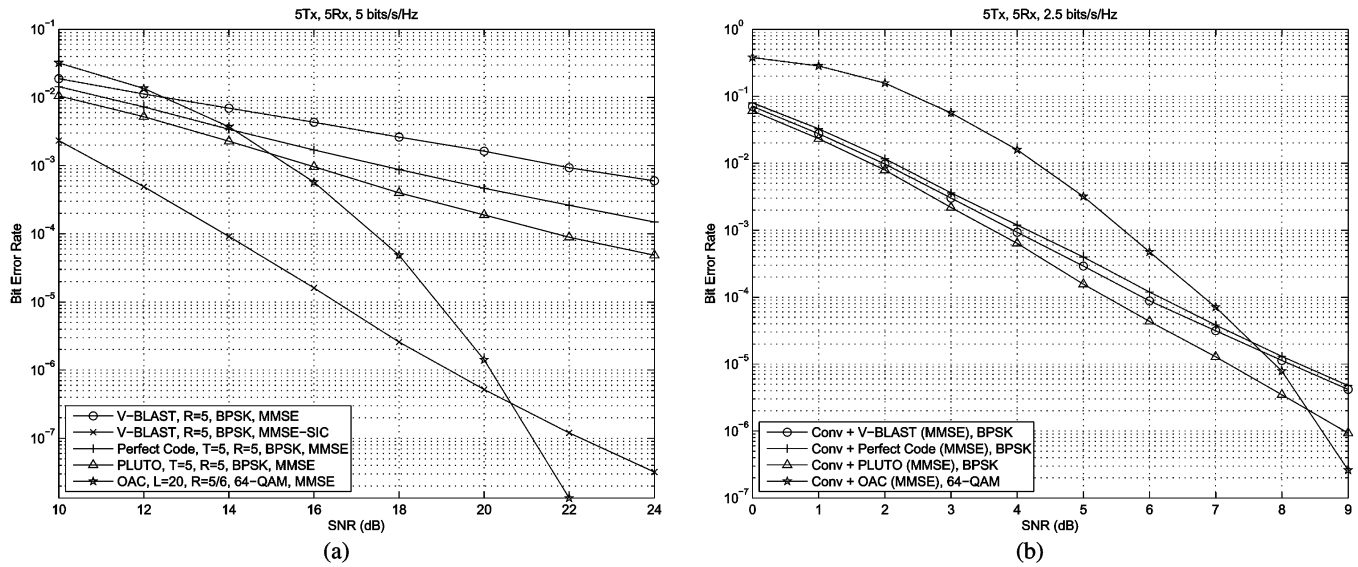

Fig. 6. Comparison of the performances of overlapped Alamouti codes, V-BLAST, PLUTO codes and perfect codes with the same throughput for five transmit and five receive antennas: (a) without outer convolutional codes and (b) with outer convolutional codes.

$5/8$ and also the shortest known block length 54. The overlapped Alamouti code and the Toeplitz code use 64-QAM constellation while the OSTBC uses 256-QAM constellation so that they have the same throughput of 5 bits/s/Hz. As a result, an almost the same performance comparison as that in Fig. 4(a) can be observed in Fig. 5.

D. Overlapped Alamouti Codes Versus Full-Rate STBC: $M = 5$, $N = 5$

In Fig. 6(a), we compare the performances of overlapped Alamouti codes, V-BLAST, PLUTO codes [47] and perfect codes [48] for five transmit and five receive antennas, where all the codes are decoded with MMSE receiver and in addition, MMSE-SIC (ordered) receiver is also used for V-BLAST that has much higher decoding complexity. Notice that the PLUTO codes proposed in [47] are designed in terms of minimizing BER for MMSE receiver at a very high symbol rate, where the requirement of high rates is due to the Gaussian approximation of the interference terms for MMSE receiver. Also note that the perfect code has achieved the diversity-multiplexing tradeoff with ML receiver when SNR goes to infinity [49]. In the comparison, the overlapped Alamouti code uses $L = 20$ and 64-QAM constellation while all the other codes use BPSK constellation. So, they have the same throughput of 5 bits/s/Hz. In Fig. 6(a), one can clearly observe the diversity gain of the overlapped Alamouti code over others and the overlapped Alamouti code even outperforms V-BLAST with MMSE-SIC (ordered) receiver when SNR is around 20.5 dB or above, while the former has a substantially smaller decoding complexity than the latter. In fact, it is known [54] that the diversity order of V-BLAST with SIC (ordered) receiver is only $N - M + 1$ that is 1 here.

When an outer convolutional code is concatenated with the codes in Fig. 6(a), their performances are compared in Fig. 6(b), where MMSE receiver is used to extract soft outputs for all the codes. The numbers of blocks per channel change for the overlapped Alamouti code, V-BLAST, the PLUTO code and the perfect code are 1 (24 channel uses), 25 (25 channel uses), 5 (25 channel uses), and 5 (25 channel uses), respectively, and the input information bit sequence to the convolutional code has length of 300 bits. One can see in Fig. 6(b) that due to the significant diversity gain, the overlapped Alamouti code outperforms the other codes when SNR is around 8.5 dB or above. Note that a little difference from the performance comparison in Fig. 6(a) is that when concatenated with the outer convolutional code, V-BLAST is slightly superior to the perfect code in the low SNR range.

V. Conclusion

In this paper, motivated by Zhang–Liu–Wong's results on Toeplitz codes [20], [21], we proposed a criterion for STBC to achieve full diversity with ZF or MMSE receiver in an MIMO system. This criterion is verified by OSTBC for which ML decoding and ZF decoding are equivalent and both achieve full diversity. We also showed that the symbol rates of STBC under this criterion are upper bounded by 1. Then, a novel family of STBC named overlapped Alamouti codes that satisfy the proposed criterion was systematically constructed and their properties were also investigated. Overlapped Alamouti codes are close to orthogonal and their symbol rates can approach 1 for any number of transmit antennas. Simulation results were provided to compare overlapped Alamouti codes with some existing codes.

Appendix

A. Proof for Theorem 1

Here, we only show the result for ZF receiver and then Theorem 1 holds automatically for MMSE receiver since MMSE receiver is optimal among linear receivers. With component-wise

hard decision at ZF receiver, (14) can be viewed as L parallel additive white Gaussian noise (AWGN) channels and the symbol SNR ρ_l for $\hat{s}_l$ at the receiver is $\rho_l = \frac{\rho}{\mu}\frac{1}{\left((\mathcal{H}^\dagger\mathcal{H})^{-1}\right)_{l,l}}$, where $\hat{s}_l$ is the lth component of $\hat{\mathbf{s}}_{ZF}$ and $(\cdot)_{l,l}$ denotes the lth diagonal element of a square matrix. If s_l is selected from some usual constellations such as PAM, PSK, or square QAM, the SEP $P_e(\hat{s}_l \to s_l|H)$ of s_l for a fixed channel matrix H is well-known in the literature that is expressed in terms of the constellation size and ρ_l. In [20], [21], a unified upper bound on $P_e(\hat{s}_l \to s_l|H)$ is derived to be

$$P_e(\hat{s}_l \to s_l|H) \le \frac{\eta-1}{\eta}\exp(-a\rho_l) \tag{47}$$

by using the alternative expressions for Gaussian $\mathcal{Q}$-function and $\mathcal{Q}^2$-function [50], [51, Ch. 4], where $a = \frac{3}{2(\eta^2-1)}$, $\frac{\sin^2(\pi/\eta)}{2}$ and $\frac{3}{4(\eta-1)}$ for PAM, PSK and square QAM constellations of cardinality η, respectively. Now, we are ready to give the following proof for Theorem 1, which is similar to the proof of the full diversity property of Toeplitz codes with linear receivers in [20], [21].

Proof: Without loss of generality, we assume $\|H\| \neq 0$ in the following proof. Let $\tilde{\mathcal{H}} = \|H\|^{-1}\mathcal{H}$, $\tilde{\mathcal{R}} = \tilde{\mathcal{H}}^\dagger\tilde{\mathcal{H}}$ and $\mathcal{R} = \mathcal{H}^\dagger\mathcal{H}$. So, $\tilde{\mathcal{R}} = \|H\|^{-2}\mathcal{R}$ and from the condition (16), we have $\|\tilde{\mathcal{H}}\| \le g$ and $\det(\tilde{\mathcal{R}}) = \|H\|^{-2L}\det(\mathcal{R}) \ge c > 0$. Hence, $\tilde{\mathcal{R}}$ must be a positive definite matrix and $\tilde{\mathcal{R}}^{-1}$ exists which is also positive definite. Let $0 < \lambda_{\min}(\tilde{\mathcal{R}}) = \lambda_1(\tilde{\mathcal{R}}) \le \lambda_2(\tilde{\mathcal{R}}) \le \cdots \le \lambda_L(\tilde{\mathcal{R}}) = \lambda_{\max}(\tilde{\mathcal{R}})$ be the L ordered eigenvalues of $\tilde{\mathcal{R}}$ and correspondingly, $\lambda_{\min}(\tilde{\mathcal{R}}^{-1})$ and $\lambda_{\max}(\tilde{\mathcal{R}}^{-1})$ be the minimum and the maximum eigenvalues of $\tilde{\mathcal{R}}^{-1}$, respectively. Then, $\sum_{i=1}^{L}\lambda_i(\tilde{\mathcal{R}}) = tr(\tilde{\mathcal{R}}) = \|\tilde{\mathcal{H}}\|^2 \le g^2$ and $\prod_{i=1}^{L}\lambda_i(\tilde{\mathcal{R}}) = \det(\tilde{\mathcal{R}}) \ge c$. So,

$$\begin{aligned}\lambda_{\max}(\tilde{\mathcal{R}}^{-1}) = \lambda_1^{-1}(\tilde{\mathcal{R}}) &\le \frac{\prod_{i=2}^{L}\lambda_i(\tilde{\mathcal{R}})}{c} \\ &\le \frac{1}{c}\left(\frac{\sum_{i=2}^{L}\lambda_i(\tilde{\mathcal{R}})}{L-1}\right)^{L-1} \\ &< \frac{1}{c}\left(\frac{g^2}{L-1}\right)^{L-1} \triangleq c_1,\end{aligned} \tag{48}$$

where the second inequality follows from the arithmetic-geometric means inequality. Note that c_1 in (48) only depends on c, g and L and hence is independent of the channel matrix H and the SNR ρ at each receive antenna. Since $\tilde{\mathcal{R}}^{-1}$ is a positive define matrix, we know $0 < \lambda_{\min}(\tilde{\mathcal{R}}^{-1}) \le (\tilde{\mathcal{R}}^{-1})_{l,l} \le \lambda_{\max}(\tilde{\mathcal{R}}^{-1}) \le c_1$.

From the above result, the receiver SNR ρ_l of $\hat{s}_l$ is lower bounded by

$$\rho_l = \frac{\rho}{\mu}\frac{1}{(\mathcal{R}^{-1})_{l,l}} = \frac{\rho}{\mu}\frac{\|H\|^2}{(\tilde{\mathcal{R}}^{-1})_{l,l}} \ge \frac{\rho\|H\|^2}{\mu c_1} = \hat{c}\rho\|H\|^2 \tag{49}$$

by letting $\hat{c} = (\mu c_1)^{-1} > 0$ that is also independent of H and ρ. Substituting (49) into (47), we have

$$P_e(\hat{s}_l \to s_l|H) \le \frac{\eta-1}{\eta}\exp(-a\hat{c}\rho\|H\|^2) \tag{50}$$

for $l = 1, 2, \ldots, L$. It has been assumed that the channel matrix H (or its vectorized version $\vec{\mathbf{h}} = (h_{1,1}, \ldots, h_{M,1}, \ldots, h_{1,N}, \ldots, h_{M,N})^t$ of length MN) is zero-mean, complex Gaussian distributed with the covariance matrix Σ. Taking the expectation of $P_e(\hat{s}_l \to s_l|H)$ over H (or, equivalently, over $\vec{\mathbf{h}}$), we obtain from (50)

$$\begin{aligned}P_e(\hat{s}_l \to s_l) &= \mathbb{E}_H\left(P_e(\hat{s}_l \to s_l|H)\right) \\ &\le \frac{\eta-1}{\eta}\frac{1}{(\pi)^{MN}\det(\Sigma)} \\ &\quad \times \int \exp(-a\hat{c}\rho\|H\|^2)\exp\left(-\vec{\mathbf{h}}^\dagger\Sigma^{-1}\vec{\mathbf{h}}\right)d\vec{\mathbf{h}} \\ &= \frac{\eta-1}{\eta}\frac{1}{(\pi)^{MN}\det(\Sigma)} \\ &\quad \times \int \exp\left(-\vec{\mathbf{h}}^\dagger(a\hat{c}\rho I_{MN} + \Sigma^{-1})\vec{\mathbf{h}}\right)d\vec{\mathbf{h}} \qquad (51) \\ &= \frac{\eta-1}{\eta}\det(\Sigma^{-1})\det((a\hat{c}\rho I_{MN} + \Sigma^{-1})^{-1}) \\ &= \frac{\eta-1}{\eta}(\det(a\hat{c}\rho\Sigma + I_{MN}))^{-1} \\ &\le \frac{\eta-1}{\eta}(\det(a\hat{c}\rho\Sigma))^{-1} \qquad (52) \\ &= \left(\frac{\eta-1}{\eta}(\det(\Sigma))^{-1}(a\hat{c})^{-MN}\right)\rho^{-MN} \qquad (53)\end{aligned}$$

where (51) follows from $\|H\|^2 = \vec{\mathbf{h}}^\dagger\vec{\mathbf{h}}$ and (52) follows from the fact that Σ and thus $a\hat{c}\rho\Sigma$ are positive definite. Since the negative exponential of the SNR ρ is MN and other terms are independent of ρ in (53), $\mathcal{X}$ achieves full diversity with ZF receiver. □

B. Proof of the Inequality (20)

Proof: Without loss of generality, we assume $\mathbf{h} = (h_1, h_2)^t \neq 0$, i.e., $\mathbf{h}$ is not an all-zero vector. The $(L+1)\times L$ Toeplitz matrix $T(\mathbf{h}, 2, L)$ has the form of

$$T(\mathbf{h}, 2, L) = \left(\begin{array}{cccc} h_1 & 0 & \ldots & 0 \\ \hline h_2 & h_1 & \ldots & 0 \\ 0 & h_2 & \ldots & 0 \\ \vdots & \vdots & \ddots & \vdots \\ 0 & 0 & \ldots & h_1 \\ \hline 0 & 0 & \ldots & h_2 \end{array}\right).$$

Since $\|\mathbf{h}\|^2 = |h_1|^2 + |h_2|^2$, either $|h_1|^2 \ge \frac{\|\mathbf{h}\|^2}{2}$ or $|h_2|^2 \ge \frac{\|\mathbf{h}\|^2}{2}$. If $|h_1|^2 \ge \frac{\|\mathbf{h}\|^2}{2}$, we write $T(\mathbf{h}, 2, L) = (T_1^t(\mathbf{h}, 2, L), T_2^t(\mathbf{h}, 2, L))^t$ with $T_1(\mathbf{h}, 2, L)$ composed of the first L rows of $T(\mathbf{h}, 2, L)$ and $T_2(\mathbf{h}, 2, L) = (0, \ldots, 0, h_2)$ being the last row of $T(\mathbf{h}, 2, L)$. So, from (17), we have

$$\begin{aligned}\det\left(T^\dagger(\mathbf{h}, 2, L)T(\mathbf{h}, 2, L)\right) &\ge \det\left(T_1^\dagger(\mathbf{h}, 2, L)T_1(\mathbf{h}, 2, L)\right) \\ &= |h_1|^{2L} \ge 2^{-L}\|\mathbf{h}\|^{2L}.\end{aligned}$$

The proof for the case of $|h_2|^2 \ge \frac{\|\mathbf{h}\|^2}{2}$ is similar except that $T_1(\mathbf{h}, 2, L)$ is now the first row of $T(\mathbf{h}, 2, L)$, i.e., the row vector $(h_1, 0, \ldots, 0)$, and $T_2(\mathbf{h}, 2, L)$ is composed of the last L rows of $T(\mathbf{h}, 2, L)$. □

C. Proof of Theorem 2

Proof: Without loss of generality, we assume $\mathbf{h}$ is not an all-zero vector and $L \geq 2$. First, we write $\mathcal{H}$ as the summation of two matrices by defining matrix $\mathcal{H}_o = \mathcal{H}|_{h_2=h_4=\cdots=h_{M-1}=0}$ and matrix $\mathcal{H}_e = \mathcal{H} - \mathcal{H}_o = \mathcal{H}|_{h_1=h_3=\cdots=h_M=0}$. From the structure of the matrix $F(\cdot,\cdot,\cdot)$ in (29), we can easily show that the matrix $\mathcal{H}_o^\dagger \mathcal{H}_e$ is skew-Hermitian, i.e., $\mathcal{H}_o^\dagger \mathcal{H}_e = -(\mathcal{H}_o^\dagger \mathcal{H}_e)^\dagger = -\mathcal{H}_e^\dagger \mathcal{H}_o$, and thus

$$\begin{aligned}\mathcal{H}^\dagger\mathcal{H} &= (\mathcal{H}_o + \mathcal{H}_e)^\dagger(\mathcal{H}_o + \mathcal{H}_e)\\ &= \mathcal{H}_o^\dagger\mathcal{H}_o + \mathcal{H}_o^\dagger\mathcal{H}_e + \mathcal{H}_e^\dagger\mathcal{H}_o + \mathcal{H}_e^\dagger\mathcal{H}_e\\ &= \mathcal{H}_o^\dagger\mathcal{H}_o + \mathcal{H}_e^\dagger\mathcal{H}_e. \end{aligned} \tag{54}$$

Below we prove the conclusion by considering even and odd L, respectively, for $\mathcal{H} = F(\mathbf{h}, M, L)$.

a) Even L. To describe the structure of $\mathcal{H}_o^\dagger\mathcal{H}_o$ and $\mathcal{H}_e^\dagger\mathcal{H}_e$, we define $\mathbf{h}_o = \left(h_M^*, h_{M-2}^*, \ldots, h_1^*\right)^t$ and $\mathbf{h}_e = (h_2, h_4, \ldots, h_{M-1})^t$, i.e., the vectors consisted of the components of $\mathbf{h}$ with odd and even indices, respectively, where $\mathbf{h}_o$ and $\mathbf{h}_e$ have lengths $\frac{M+1}{2}$ and $\frac{M-1}{2}$, respectively. Note that the indices are in a decreasing order in $\mathbf{h}_o$. From the structure of $F(\mathbf{h}, M, L)$, it is not hard to verify

$$\mathcal{H}_o^\dagger\mathcal{H}_o = \left(T^\dagger\left(\mathbf{h}_o, \frac{M+1}{2}, \frac{L}{2}\right) T\left(\mathbf{h}_o, \frac{M+1}{2}, \frac{L}{2}\right)\right) \otimes I_2 \tag{55}$$

and

$$\mathcal{H}_e^\dagger\mathcal{H}_e = \left(T^\dagger\left(\mathbf{h}_e, \frac{M-1}{2}, \frac{L}{2}\right) T\left(\mathbf{h}_e, \frac{M-1}{2}, \frac{L}{2}\right)\right) \otimes I_2 \tag{56}$$

for even L, where $T(\cdot,\cdot,\cdot)$ is the Toeplitz matrix defined in (10) and $\otimes$ denotes the Kronecker product between two matrices. It has been shown in Lemma 1 that there exist two positive constants c_o and c_e that are independent of $\mathbf{h}_o$ and $\mathbf{h}_e$, respectively, such that

$$\det\left(T^\dagger\left(\mathbf{h}_o, \frac{M+1}{2}, \frac{L}{2}\right) T\left(\mathbf{h}_o, \frac{M+1}{2}, \frac{L}{2}\right)\right) \geq c_o\|\mathbf{h}_o\|^L \tag{57}$$

and

$$\det\left(T^\dagger\left(\mathbf{h}_e, \frac{M-1}{2}, \frac{L}{2}\right) T\left(\mathbf{h}_e, \frac{M-1}{2}, \frac{L}{2}\right)\right) \geq c_e\|\mathbf{h}_e\|^L$$

for any $\mathbf{h}_o$ and $\mathbf{h}_e$, respectively. Hence

$$\begin{aligned}&\det\left(\mathcal{H}_o^\dagger\mathcal{H}_o\right)\\ &= \left(\det\left(T^\dagger\left(\mathbf{h}_o, \frac{M+1}{2}, \frac{L}{2}\right) T\left(\mathbf{h}_o, \frac{M+1}{2}, \frac{L}{2}\right)\right)\right)^2\\ &\geq c_o^2\|\mathbf{h}_o\|^{2L}\end{aligned} \tag{58}$$

[53, p. 48] and similarly, $\det(\mathcal{H}_e^\dagger\mathcal{H}_e) \geq c_e^2\|\mathbf{h}_e\|^{2L}$. Note that c_o and c_e do not depend on $\mathbf{h}$. Now, we consider the following two cases regarding to $\|\mathbf{h}_o\|$.

i) $\|\mathbf{h}_o\|^2 \geq \frac{1}{2}\|\mathbf{h}\|^2$. For any $\mathbf{h}$, we have from (17), (54) and (58) that

$$\det(\mathcal{H}^\dagger\mathcal{H}) \geq \det\left(\mathcal{H}_o^\dagger\mathcal{H}_o\right) \geq c_o^2\|\mathbf{h}_o\|^{2L} \geq 2^{-L}c_o^2\|\mathbf{h}\|^{2L}.$$

ii) $\|\mathbf{h}_o\|^2 < \frac{1}{2}\|\mathbf{h}\|^2$. Then, $\|\mathbf{h}_e\|^2 \geq \frac{1}{2}\|\mathbf{h}\|^2$ and similar to the derivation in case i), we have

$$\det(\mathcal{H}^\dagger\mathcal{H}) \geq \det\left(\mathcal{H}_e^\dagger\mathcal{H}_e\right) \geq c_e^2\|\mathbf{h}_e\|^{2L} \geq 2^{-L}c_e^2\|\mathbf{h}\|^{2L}.$$

Therefore, by letting $c_L = 2^{-L}\min(c_o^2, c_e^2)$ that is independent of $\mathbf{h}$, we have $\det(\mathcal{H}^\dagger\mathcal{H}) \geq c_L\|\mathbf{h}\|^{2L}$ and thus prove the conclusion for even L.

b) Odd L. For any given channel matrix (vector) $\mathbf{h}$, we have

$$\mathcal{H}_{(L+1)}^\dagger\mathcal{H}_{(L+1)} = \left(\begin{array}{c|c} \mathcal{H}_{(L)}^\dagger\mathcal{H}_{(L)} & \mathbf{t} \\ \hline \mathbf{t}^\dagger & \|\mathbf{h}\|^2 \end{array}\right) \tag{59}$$

where, for simplicity, we write $\mathcal{H}_{(L+1)}$ and $\mathcal{H}_{(L)}$ to denote $F(\mathbf{h}, M, L+1)$ and $F(\mathbf{h}, M, L)$, respectively, and $\mathbf{t}$ is a vector of length L.

Since $L+1$ is even, we have shown in part a) that

$$\det\left(\mathcal{H}_{(L+1)}^\dagger\mathcal{H}_{(L+1)}\right) \geq c_{L+1}\|\mathbf{h}\|^{2L+2} \tag{60}$$

for some positive constant c_{L+1} that is independent of $\mathbf{h}$. So, $\mathcal{H}_{(L+1)}^\dagger\mathcal{H}_{(L+1)}$ is positive definite and we use $0 < \lambda_1(\mathcal{H}_{(L+1)}^\dagger\mathcal{H}_{(L+1)}) \leq \lambda_2(\mathcal{H}_{(L+1)}^\dagger\mathcal{H}_{(L+1)}) \leq \cdots \leq \lambda_{L+1}(\mathcal{H}_{(L+1)}^\dagger\mathcal{H}_{(L+1)})$ to denote the $L+1$ ordered eigenvalues of $\mathcal{H}_{(L+1)}^\dagger\mathcal{H}_{(L+1)}$. Correspondingly, let $\lambda_1(\mathcal{H}_{(L)}^\dagger\mathcal{H}_{(L)}) \leq \lambda_2(\mathcal{H}_{(L)}^\dagger\mathcal{H}_{(L)}) \leq \cdots \leq \lambda_L(\mathcal{H}_{(L)}^\dagger\mathcal{H}_{(L)})$ be the L ordered eigenvalues of $\mathcal{H}_{(L)}^\dagger\mathcal{H}_{(L)}$. Then, from [55, Th. 4.3.8, p. 185], we have

$$\begin{aligned}0 &< \lambda_i\left(\mathcal{H}_{(L+1)}^\dagger\mathcal{H}_{(L+1)}\right) \leq \lambda_i\left(\mathcal{H}_{(L)}^\dagger\mathcal{H}_{(L)}\right)\\ &\leq \lambda_{i+1}\left(\mathcal{H}_{(L+1)}^\dagger\mathcal{H}_{(L+1)}\right), \quad i = 1, 2, \ldots, L.\end{aligned} \tag{61}$$

Since $\sum_{i=1}^{L+1}\lambda_i\left(\mathcal{H}_{(L+1)}^\dagger\mathcal{H}_{(L+1)}\right) = tr\left(\mathcal{H}_{(L+1)}^\dagger\mathcal{H}_{(L+1)}\right) = (L+1)\|\mathbf{h}\|^2$ that implies $\lambda_{L+1}(\mathcal{H}_{(L+1)}^\dagger\mathcal{H}_{(L+1)}) < (L+1)\|\mathbf{h}\|^2$, we have

$$\begin{aligned}\det\left(\mathcal{H}_{(L)}^\dagger\mathcal{H}_{(L)}\right) &= \prod_{i=1}^{L}\lambda_i\left(\mathcal{H}_{(L)}^\dagger\mathcal{H}_{(L)}\right)\\ &\geq \prod_{i=1}^{L}\lambda_i\left(\mathcal{H}_{(L+1)}^\dagger\mathcal{H}_{(L+1)}\right)\\ &= \frac{\det\left(\mathcal{H}_{(L+1)}^\dagger\mathcal{H}_{(L+1)}\right)}{\lambda_{L+1}\left(\mathcal{H}_{(L+1)}^\dagger\mathcal{H}_{(L+1)}\right)}\end{aligned}$$

$$> \frac{\det\left(\mathcal{H}_{(L+1)}^{\dagger}\mathcal{H}_{(L+1)}\right)}{(L+1)\|\mathbf{h}\|^2} \geq \frac{c_{L+1}\|\mathbf{h}\|^{2L+2}}{(L+1)\|\mathbf{h}\|^2} = \frac{c_{L+1}}{L+1}\|\mathbf{h}\|^{2L}$$

where the first inequality follows from (61) and the last inequality follows from (60). Since $\frac{c_{L+1}}{L+1}$ is a positive constant independent of $\mathbf{h}$, we have thus completed the proof. □

D. Proof of the Inequality (33)

Proof: Without loss of generality, we assume $\mathbf{h} = (h_1, h_2, h_3)^t$ is not an all-zero vector and $L \geq 2$. Like the proof of Theorem 2 in Appendix C, we consider the cases for even and odd L, respectively.

a) Even L. Still using the notations and symbols in Appendix C, $\mathcal{H} = F(\mathbf{h}, 3, L)$, we have

$$\mathcal{H}^{\dagger}\mathcal{H} = \mathcal{H}_o^{\dagger}\mathcal{H}_o + \mathcal{H}_e^{\dagger}\mathcal{H}_e = \left(T^{\dagger}(\mathbf{h}_o, 2, L/2)T(\mathbf{h}_o, 2, L/2) + |h_2|^2 I_{\frac{L}{2}}\right) \otimes I_2 \quad (62)$$

from (54) to (56), where $\mathbf{h}_o = (h_3^*, h_1^*)^t$. Consider the following two cases regarding to $|h_2|$.

i) $|h_2|^2 \geq \frac{1}{3}\|\mathbf{h}\|^2$. Then, from (17)

$$\det\left(T^{\dagger}(\mathbf{h}_o, 2, L/2)T(\mathbf{h}_o, 2, L/2) + |h_2|^2 I_{\frac{L}{2}}\right) \geq \det\left(|h_2|^2 I_{\frac{L}{2}}\right) \geq 3^{-\frac{L}{2}}\|\mathbf{h}\|^L.$$

ii) $|h_2|^2 < \frac{1}{3}\|\mathbf{h}\|^2$. Then, $\|\mathbf{h}_o\|^2 \geq \frac{2}{3}\|\mathbf{h}\|^2$ and hence

$$\begin{aligned}&\det\left(T^{\dagger}(\mathbf{h}_o, 2, L/2)T(\mathbf{h}_o, 2, L/2) + |h_2|^2 I_{\frac{L}{2}}\right)\\ &\quad \geq \det\left(T^{\dagger}(\mathbf{h}_o, 2, L/2)T(\mathbf{h}_o, 2, L/2)\right)\\ &\quad \geq 2^{-\frac{L}{2}}\|\mathbf{h}_o\|^L \geq 3^{-\frac{L}{2}}\|\mathbf{h}\|^L\end{aligned}$$

where the second inequality follows from (20).

For both of the above cases, we have from (62) that $\det\left(\mathcal{H}^{\dagger}\mathcal{H}\right) \geq \left(3^{-\frac{L}{2}}\|\mathbf{h}\|^L\right)^2 = 3^{-L}\|\mathbf{h}\|^{2L} = 3^{-L-(L \bmod 2)}\|\mathbf{h}\|^{2L}$ [53, p. 48] because L is even. Thus, we have proved the result for even L case.

b) Odd L. As in the the proof of Theorem 2, for any given $\mathbf{h}$, we use $\mathcal{H}_{(l)}$ to denote the matrix $F(\mathbf{h}, 3, l)$ of l columns, $l \geq 1$. So, like (59), we can write

$$\mathcal{H}_{(L)}^{\dagger}\mathcal{H}_{(L)} = \left(\begin{array}{c|c} \mathcal{H}_{(L-1)}^{\dagger}\mathcal{H}_{(L-1)} & \mathbf{t} \\ \hline \mathbf{t}^{\dagger} & \|\mathbf{h}\|^2 \end{array}\right) \quad (63)$$

with $\mathbf{t} = (0, \ldots, 0, h_1^* h_3, 0)^t$ of length $L-1$. For a partitioned matrix

$$M = \left(\begin{array}{c|c} M_1 & M_2 \\ \hline M_3 & M_4 \end{array}\right)$$

with square submatrices M_1 and M_4, we have [53, p. 50]

$$\det(M) = \det(M_4)\det(M_1 - M_2 M_4^{-1} M_3) \quad (64)$$

if M_4 is invertible. Therefore, we know from (63) that

$$\det\left(\mathcal{H}_{(L)}^{\dagger}\mathcal{H}_{(L)}\right) = \|\mathbf{h}\|^2 \det\underbrace{\left(\mathcal{H}_{(L-1)}^{\dagger}\mathcal{H}_{(L-1)} - \|\mathbf{h}\|^{-2}\mathbf{t}\mathbf{t}^{\dagger}\right)}_{\mathcal{R}_{(L-1)}^{(1)}}. \quad (65)$$

On the other hand, we can write

$$\mathcal{H}_{(L+1)}^{\dagger}\mathcal{H}_{(L+1)} = \left(\begin{array}{c|cc} \mathcal{H}_{(L-1)}^{\dagger}\mathcal{H}_{(L-1)} & \mathbf{t} & \hat{\mathbf{t}} \\ \hline \mathbf{t}^{\dagger} & \|\mathbf{h}\|^2 & 0 \\ \hat{\mathbf{t}}^{\dagger} & 0 & \|\mathbf{h}\|^2 \end{array}\right)$$

with $\hat{\mathbf{t}} = (0, \ldots, 0, h_1^* h_3)^t$ of length $L-1$, and thus according to (64)

$$\det\left(\mathcal{H}_{(L+1)}^{\dagger}\mathcal{H}_{(L+1)}\right) = \|\mathbf{h}\|^4 \det\underbrace{\left(\mathcal{H}_{(L-1)}^{\dagger}\mathcal{H}_{(L-1)} - \|\mathbf{h}\|^{-2}\mathbf{t}\mathbf{t}^{\dagger} - \|\mathbf{h}\|^{-2}\hat{\mathbf{t}}\hat{\mathbf{t}}^{\dagger}\right)}_{\mathcal{R}_{(L-1)}^{(2)} = \mathcal{R}_{(L-1)}^{(1)} - \|\mathbf{h}\|^{-2}\hat{\mathbf{t}}\hat{\mathbf{t}}^{\dagger}}. \quad (66)$$

Since $L+1$ is even, we have shown in part a) that $\det\left(\mathcal{H}_{(L+1)}^{\dagger}\mathcal{H}_{(L+1)}\right) \geq 3^{-(L+1)}\|\mathbf{h}\|^{2L+2}$ and hence

$$\det\left(\mathcal{R}_{(L-1)}^{(2)}\right) \geq 3^{-(L+1)}\|\mathbf{h}\|^{2L-2} \quad (67)$$

from (66), implying $\mathcal{R}_{(L-1)}^{(2)}$ is a positive definite matrix. So, according to (17),

$$\det\left(\mathcal{R}_{(L-1)}^{(1)}\right) = \det\left(\mathcal{R}_{(L-1)}^{(2)} + \|\mathbf{h}\|^{-2}\hat{\mathbf{t}}\hat{\mathbf{t}}^{\dagger}\right) \geq \det\left(\mathcal{R}_{(L-1)}^{(2)}\right) \quad (68)$$

as matrix $\|\mathbf{h}\|^{-2}\hat{\mathbf{t}}\hat{\mathbf{t}}^{\dagger}$ is positive semidefinite. Hence, we have from (65), (67) and (68) that

$$\begin{aligned}\det\left(\mathcal{H}_{(L)}^{\dagger}\mathcal{H}_{(L)}\right) &= \|\mathbf{h}\|^2 \det\left(\mathcal{R}_{(L-1)}^{(1)}\right)\\ &\geq \|\mathbf{h}\|^2 \det\left(\mathcal{R}_{(L-1)}^{(2)}\right) \geq 3^{-(L+1)}\|\mathbf{h}\|^{2L}\\ &= 3^{-L-(L \bmod 2)}\|\mathbf{h}\|^{2L}\end{aligned}$$

because L is odd, and we have thus completed the proof.

ACKNOWLEDGMENT

The authors would like to thank Jing Liu, Jian-Kang Zhang, and Max Wong for sending them the manuscript [21] and having useful discussions on Toeplitz codes. The authors would also like to thank the anonymous reviewers for their detailed and helpful comments to improve the presentation of this paper.

REFERENCES

[1] N. Seshadri and J. H. Winters, "Two signaling schemes for improving the error performance of frequency-division-duplex (FDD) transmission systems using transmitter antenna diversity," *Int. J. Wireless Inf. Netw.*, vol. 1, no. 1, pp. 49–60, Jan. 1994.

[2] J.-C. Guey, M. P. Fitz, M. R. Bell, and W.-Y. Kuo, "Signal design for transmitter diversity wireless communication systems over Rayleigh fading channels," *IEEE Trans. Commun.*, vol. 47, pp. 527–537, Apr. 1999.

[3] V. Tarokh, N. Seshadri, and A. R. Calderbank, "Space-time codes for high data rate wireless communication: Performance criterion and code construction," *IEEE Trans. Inf. Theory*, vol. 44, pp. 744–765, Mar. 1998.

[4] S. M. Alamouti, "A simple transmit diversity technique for wireless communications," *IEEE J. Sel. Areas Commun.*, vol. 16, pp. 1451–1458, Oct. 1998.

[5] V. Tarokh, H. Jafarkhani, and A. R. Calderbank, "Space-time block codes from orthogonal designs," *IEEE Trans. Inf. Theory*, vol. 45, pp. 1456–1467, Jul. 1999.

[6] G. Ganesan and P. Stoica, "Space-time block codes: A maximum SNR approach," *IEEE Trans. Inf. Theory*, vol. 47, pp. 1650–1656, May 2001.

[7] H. Wang and X.-G. Xia, "Upper bounds of rates of complex orthogonal space-time block codes," *IEEE Trans. Inf. Theory*, vol. 49, pp. 2788–2796, Oct. 2003.

[8] X.-B. Liang, "Orthogonal designs with maximal rates," *IEEE Trans. Inf. Theory*, vol. 49, pp. 2468–2503, Oct. 2003.

[9] W. Su, X.-G. Xia, and K. J. R. Liu, "A systematic design of high-rate complex orthogonal space-time block codes," *IEEE Commun. Lett.*, vol. 8, pp. 380–382, Jun. 2004.

[10] K. Lu, S. Fu, and X.-G. Xia, "Closed-form designs of complex orthogonal space-time block codes of rates $(2k+1)/(2k)$ for $2k-1$ or $2k$ transmit antennas," *IEEE Trans. Inf. Theory*, vol. 51, pp. 4340–4347, Dec. 2005.

[11] W. Su, S. N. Batalama, and D. A. Pados, "On orthogonal space-time block codes and transceiver signal linearization," *IEEE Commun. Lett.*, vol. 10, pp. 91–93, Feb. 2006.

[12] H. Jafarkhani, "A quasi-orthogonal space-time block codes," *IEEE Trans. Commun.*, vol. 49, pp. 1–4, Jan. 2001.

[13] O. Tirkkonen, A. Boariu, and A. Hottinen, "Minimal non-orthogonality rate 1 space-time block code for 3-Tx antennas," in *Proc. IEEE Int. Symp. Spread Spectrum Tech. Appl. (ISSSTA'00)*, NJ, Sep. 6–8, 2000, pp. 429–432.

[14] C. B. Papadias and G. J. Foschini, "Capacity-approaching space-time codes for systems employing four transmitter antennas," *IEEE Trans. Inf. Theory*, vol. 49, pp. 726–732, Mar. 2003.

[15] N. Sharma and C. B. Papadias, "Improved quasi-orthogonal codes through constellation rotation," *IEEE Trans. Commun.*, vol. 51, pp. 332–335, Mar. 2003.

[16] W. Su and X.-G. Xia, "Signal constellations for quasi-orthogonal space-time block codes with full diversity," *IEEE Trans. Inf. Theory*, vol. 50, pp. 2331–2347, Oct. 2004.

[17] Z. A. Khan and B. S. Rajan, "Single-symbol maximum likelihood decodable linear STBCs," *IEEE Trans. Inf. Theory*, vol. 52, pp. 2062–2091, May 2006.

[18] C. Yuen, Y. L. Guan, and T. T. Tjhung, "Quasi-orthogonal STBC with minimum decoding complexity," *IEEE Trans. Wireless Commun.*, vol. 4, no. 5, pp. 2089–2094, Sep. 2005.

[19] H. Wang, D. Wang, and X.-G. Xia, "On optimal quasi-orthogonal space-time block codes with minimum decoding complexity," in *Proc. IEEE Int. Symp. Inf. Theory (ISIT'05)*, Adelaide, Australia, Sep. 4–9, 2005, pp. 1168–1172.

[20] J.-K. Zhang, J. Liu, and K. M. Wong, "Linear Toeplitz space time block codes," in *Proc. IEEE Int. Symp. Inf. Theory (ISIT'05)*, Adelaide, Australia, Sep. 4–9, 2005, pp. 1942–1946.

[21] J. Liu, J.-K. Zhang, and K. M. Wong, "Properties and applications of the Toeplitz space-time block codes," *IEEE Trans. Inf. Theory*, to be published.

[22] B. Hassibi and B. M. Hochwald, "High-rate codes that are linear in space and time," *IEEE Trans. Inf. Theory*, vol. 48, pp. 1804–1824, Jul. 2002.

[23] R. W. Heath and A. J. Paulraj, "Linear dispersion codes for MIMO systems based on frame theory," *IEEE Trans. Signal Process.*, vol. 50, no. 10, pp. 2429–2441, Oct. 2002.

[24] E. Viterbo and E. Biglieri, "A universal lattice decoder," in *GRETSI 14-ème Colloque*, Juan-les-Pins, France, Sep. 1993, pp. 611–614.

[25] E. Viterbo and J. Boutros, "A universal lattice code decoder for fading channel," *IEEE Trans. Inf. Theory*, vol. 45, pp. 1639–1642, Jul. 1999.

[26] M. O. Damen, K. Abed-Meraim, and J. C. Belfiore, "Generalized sphere decoder for asymmetrical space-time communication architecture," *Inst. Elec. Electr. Electron. Lett.*, vol. 36, no. 2, pp. 166–166, Jan. 2000.

[27] M. O. Damen, A. Chkeif, and J. C. Belfiore, "Lattice code decoder for space-time codes," *IEEE Commun. Lett.*, vol. 4, pp. 161–163, May 2000.

[28] B. M. Hochwald and S. ten Brink, "Achieving near-capacity on a multiple-antenna channel," *IEEE Trans. Commun.*, vol. 51, pp. 389–399, Mar. 2003.

[29] B. Hassibi and H. Vikalo, "On the sphere decoding algorithm I. expected complexity," *IEEE Trans. Signal Process.*, vol. 53, no. 8, pp. 2806–2818, Aug. 2005.

[30] B. Hassibi and H. Vikalo, "On the sphere decoding algorithm II. Generalizations, second-order statistics, and applications to communications," *IEEE Trans. Signal Process.*, vol. 53, no. 8, pp. 2819–2834, Aug. 2005.

[31] W. H. Mow, "Universal lattice decoding: principle and recent advances," *Wireless Commun. Mobile Comput.*, vol. 3, no. 5, pp. 553–569, Aug. 2003.

[32] J. Hagenauer, "Forward error correcting for CDMA systems," in *Proc. IEEE Int. Symp. Spread Spectrum Tech. Appl. (ISSSTA'96)*, Mainz, Germany, Sep. 22–25, 1996, pp. 566–569.

[33] X. Wang and H. V. Poor, "Iterative (turbo) soft interference cancellation and decoding for coded CDMA," *IEEE Trans. Commun.*, vol. 47, pp. 1046–1061, Jul. 1999.

[34] H. V. Poor and S. Verdú, "Probability of error in MMSE multiuser detection," *IEEE Trans. Inf. Theory*, vol. 43, pp. 858–871, May 1997.

[35] W.-J. Choi, K.-W. Cheong, and J. M. Cioffi, "Iterative soft interference cancellation for multiple antenna systems," in *Proc. IEEE Wireless Commun. Network. Conf. (WCNC'00)*, Chicago, IL, USA, Sep. 23–28, 2000, pp. 304–309.

[36] P. Li, L. Liu, K. Y. Wu, and W. K. Leung, "A unified approach to multiuser detection and space-time coding with low complexity and nearly optimal performance," in *Proc. 40th Annu. Allerton Conf. Commun., Contr., Comput.*, Monticello, IL, USA, Oct. 1–3, 2002, pp. 170–179.

[37] P. Li, "Interleave-division multiple access and chip-by-chip iterative multi-user detection," *IEEE Radio Commun.*, pp. S19–S23, Jun. 2005.

[38] Y. Li and X.-G. Xia, "Iterative demodulation/decoding methods based on Gaussian approximations for lattice based space-time coded systems," *IEEE Trans. Wireless Commun.*, vol. 5, no. 8, pp. 1976–1983, Aug. 2006.

[39] P. Patel and J. Holtzman, "Analysis of a simple successive interference cancellation scheme in DS/CDMA system," *IEEE J. Sel. Areas Commun.*, vol. 12, pp. 796–807, Jun. 1994.

[40] G. D. Golden, G. J. Foschini, R. A. Valenzuela, and P. W. Wolniansky, "Detection algorithm and initial laboratory results using V-BLAST space-time communication architecture," *Inst. Elec. Electr. Elect. Lett.*, vol. 35, no. 1, pp. 14–16, Jan. 1999.

[41] G. J. Foschini, G. D. Golden, R. A. Valenzuela, and P. W. Wolniansky, "Simplified processing for high spectral efficiency wireless communications employing multi-element arrays," *IEEE J. Sel. Area. Commun*, vol. 17, no. 11, pp. 1841–1852, Nov. 1999.

[42] A. Zanella, M. Chiani, and M. Z. Win, "MMSE reception and successive interference cancellation for MIMO systems with high spectral efficiency," *IEEE Trans. Wireless Commun.*, vol. 4, no. 3, pp. 1244–1253, May 2005.

[43] H. E. Gamal, G. Caire, and M. O. Damen, "Lattice coding and decoding achieving the optimal diversity-multiplexing tradeoff of MIMO channels," *IEEE Trans. Inf. Theory*, vol. 50, pp. 968–985, Jun. 2004.

[44] A. Medles and D. T. M. Slock, "Achieving the optimal diversity-versus-multiplexing tradeoff for MIMO flat channels with QAM space-time spreading and DFE equalization," *IEEE Trans. Inf. Theory*, vol. 52, pp. 5312–5323, Dec. 2006.

[45] L. Zheng and D. Tse, "Diversity and multiplexing: A fundamental tradeoff in multiple-antenna channels," *IEEE Trans. Inf. Theory*, vol. 49, pp. 1073–1096, May 2003.

[46] M. Fiedler, "Bounds for the determinant of the sum of Hermitian matrices," *Proc. Amer. Math. Soc.*, vol. 30, no. 1, pp. 27–31, Sep. 1971.

[47] J. Liu, J.-K. Zhang, and K. M. Wong, "On the design of minimum BER linear space-time block codes for MIMO systems equipped with MMSE receivers," *IEEE Trans. Signal Process.*, vol. 54, no. 8, pp. 3147–3158, Aug. 2006.

[48] P. Elia, B. A. Sethuraman, and P. V. Kumar, "Perfect space-time codes for any number of antennas," *IEEE Trans. Inf. Theory*, vol. 53, pp. 3853–3868, Nov. 2007.

[49] P. Elia, K. R. Kumar, S. A. Pawar, P. V. Kumar, and H.-F. Lu, "Explicit space-time codes achieving the diversity-multiplexing gain tradeoff," *IEEE Trans. Inf. Theory*, vol. 52, pp. 3869–3884, Sep. 2006.

[50] M. K. Simon and M.-S. Alouini, "A unified approach to the performance analysis of digital communication over generalized fading channels," *Proc. IEEE*, vol. 86, pp. 1860–1877, Sep. 1998.

[51] M. K. Simon and M.-S. Alouini, *Digital Communication over Fading Channels: A Unified Approach to Performance Analysis*. New York: Wiley, 2000.

[52] D. Tse and P. Viswanath, *Fundamentals of Wireless Communication*. Cambridge, U.K.: Cambridge University Press, 2005.

[53] H. Lütkepohl, *Handbook of Matrices*. New York: Wiley, 1996.

[54] S. Haykin and M. Moher, *Modern Wireless Communications*. Upper Saddle River, NJ: Prentice Hall, 2004.

[55] R. A. Horn and C. R. Johnson, *Matrix Analysis*. Cambridge, U.K.: Cambridge Univ. Press, 1985.